THE JOURNAL OF BIOLOGICAL CHEMISTRY VOL. 289, NO. 20, pp. 14089–14108, May 16, 2014

Distinct Modes of Ubiquitination of Peroxisome-targeting Signal Type 1 (PTS1) Receptor Pex5p Regulate PTS1 Protein Import*[S]

Received for publication, October 18, 2013, and in revised form, March 4, 2014 Published, JBC Papers in Press, March 24, 2014, DOI 10.1074/jbc.M113.527937

Kanji Okumoto[‡§], **Hiromi Noda**[‡], **and Yukio Fujiki**[‡1]

From the [‡]*Department of Biology, Faculty of Sciences, and the* [§]*Graduate School of Systems Life Sciences, Kyushu University Graduate School, Fukuoka 812-8581, Japan*

Background: Pex5p translocates the cargo proteins into peroxisomes.
Results: Mammalian RING peroxins, the Pex10p·Pex12p complex, catalyze Lys-linked, multiple monoubiquitination of Pex5p, assuring efficient export of Pex5p from peroxisomes.
Conclusion: Distinct Lys- and Cys-linked modes of Pex5p ubiquitination control Pex5p-mediated matrix protein import.
Significance: This work provides the first evidence of a functional role of mammalian RING peroxins in Pex5p ubiquitination.

Peroxisome targeting signal type-1 (PTS1) receptor, Pex5p, is a key player in peroxisomal matrix protein import. Pex5p recognizes PTS1 cargoes in the cytosol, targets peroxisomes, translocates across the membrane, unloads the cargoes, and shuttles back to the cytosol. Ubiquitination of Pex5p at a conserved cysteine is required for the exit from peroxisomes. However, any potential ubiquitin ligase (E3) remains unidentified in mammals. Here, we establish an *in vitro* ubiquitination assay system and demonstrate that RING finger Pex10p functions as an E3 with an E2, UbcH5C. The E3 activity of Pex10p is essential for its peroxisome-restoring activity, being enhanced by another RING peroxin, Pex12p. The Pex10p·Pex12p complex catalyzes monoubiquitination of Pex5p at one of multiple lysine residues *in vitro*, following the dissociation of Pex5p from Pex14p and the PTS1 cargo. Several lines of evidence with lysine-to-arginine mutants of Pex5p demonstrate that Pex10p RING E3-mediated ubiquitination of Pex5p is required for its efficient export from peroxisomes to the cytosol and peroxisomal matrix protein import. RING peroxins are required for both modes of Pex5p ubiquitination, thus playing a pivotal role in Pex5p shuttling.

Peroxisomal proteins, including matrix and membrane proteins, are synthesized on free polyribosomes in the cytosol and post-translationally translocated to peroxisomes (1). Two types of peroxisome-targeting signals (PTSs),[2] PTS1 (2, 3) and PTS2 (4, 5), are identified as topogenic signals for matrix proteins. In mammals, 14 *PEX* gene products, termed peroxins, have been isolated, 10 of which are involved in matrix protein import into peroxisomes (reviewed in Refs. 6 and 7). Pex5p and Pex7p are the cytosolic receptors for PTS1 and PTS2 proteins, respectively (8–12). Pex5p recognizes newly synthesized PTS1 proteins in the cytosol, and the Pex5p·cargo complexes are targeted to peroxisome membranes by docking to membrane peroxins, Pex14p and Pex13p (13–15). Pex5p then releases the cargo proteins into the peroxisomal matrix, which is mediated by the association of Pex5p with a putative import machinery, including a docking complex (Pex14p and Pex13p) and a translocation complex comprising three RING peroxins, Pex2p, Pex10p, and Pex12p (6, 7). Finally, Pex5p shuttles back to the cytosol in a manner dependent on ATP and AAA family peroxins, Pex1p and Pex6p (16, 17).

Ubiquitination is a post-translational protein modification, in which the ubiquitin-activating enzyme (E1) transfers ubiquitin to a ubiquitin-conjugating enzyme (E2), and a protein-ubiquitin ligase (E3) catalyzes transfer of the ubiquitin moiety from ubiquitin E2 to the substrate (18). Ubiquitination of Pex5p has been demonstrated in yeast and mammals and conclusively regulates Pex5p function, especially in the export from peroxisome membrane to the cytosol. Yeast genetic approaches have revealed that Pex5p is ubiquitinated in two distinct modes. Monoubiquitination at the N-terminal conserved cysteine of Pex5p is required for the recycling as well as peroxisome matrix protein import (19, 20). Polyubiquitination at the conserved two lysines of N-terminal region of Pex5p leads to the degradation of Pex5p (20–23). These two types of ubiquitin modifications at the conserved cysteine and lysine(s) with similar functions are also reported in the PTS2 co-receptors, *Saccharomyces cerevisiae* Pex18p (24) and *Pichia pastoris* Pex20p (25, 26). In mammals, a conserved cysteine near the N terminus of Pex5p (Cys^{11}) is monoubiquitinated via a thioester bond, being

* This work was supported in part by Grants-in-Aid for Scientific Research 19058011, 20370039, 24247038, and 25112518 (to Y. F.) and 1977087, 21770117, and 24770130 (to K. O.), the Global Centers of Excellence Program, and Grants for Excellent Graduate Schools from the Ministry of Education, Culture, Sports, Science, and Technology of Japan; SORST and CREST grants (to Y. F.) from the Science and Technology Agency of Japan; and grants (to Y. F.) from the Takeda Science Foundation and the Japanese Foundation for Applied Enzymology.
[S] This article contains supplemental Table S1.
[1] To whom correspondence should be addressed: Dept. of Biology, Faculty of Sciences, Kyushu University Graduate School, 6-10-1 Hakozaki, Higashi-ku, Fukuoka 812-8581, Japan. Tel.: 81-92-642-2635; Fax: 81-92-642-4214; E-mail: yfujiki@kyudai.jp.
[2] The abbreviations used are: PTS, peroxisome targeting signal; Ub, ubiquitin; HA_2-Ub, tandem HA-tagged ubiquitin; His, hexahistidine; MBP, maltose-binding protein; PBD, peroxisome biogenesis disorder; PNS, post-nuclear supernatant; K-less, lysineless; HF-Pex5pL, N-terminally His- and FLAG-tagged Chinese hamster Pex5pL; KR mutant, lysine to arginine mutant; 520K, KR mutant where all lysine residues other than Lys^{520} are mutated to arginine.

essential for Pex5p export (27–29). An E2 enzyme, yeast Pex4p, facilitates monoubiquitination of Pex5p (Cys[6] in *S. cerevisiae*) (19, 20, 30), whereas Ubc4 functions as E2 in polyubiquitination of Pex5p (21–23). The cysteine-linked ubiquitination (Cys-ubiquitination) of human Pex5p is reconstituted in the presence of E2 enzymes, UbcH5a/b/c, in a cell-free Pex5p import system (28). However, ubiquitination of Pex5p via a lysine residue is largely unknown in mammalian cells.

The RING (really interesting new gene) finger motif is found in over 300 proteins in mammals with diverse cellular functions and categorized as major E3 enzymes (31). RING peroxins Pex2p, Pex10p, and Pex12p possess similar domain structure with two transmembrane segments and a RING finger, showing the same membrane topology, in which the N-terminal and RING finger-containing C-terminal parts are exposed to the cytosol (see Fig. 2*A*) (6, 7). Deficiency of any one of the RING peroxins results in typical import defects of peroxisomal matrix proteins of both the PTS1 and PTS2 types, but not membrane proteins, as seen in *pex2*, *pex10*, and *pex12* cell mutants, including fibroblasts from patients with peroxisome biogenesis disorders (PBDs) (6, 32). Pex5p is accumulated in peroxisome remnants in RING peroxin-impaired cell mutants (14, 33), implying that RING peroxins are required at a step(s) downstream of Pex5p docking to Pex14p, most likely during the translocation of matrix proteins across the membrane (34, 35). Involvement of RING peroxins in the Pex5p ubiquitination is shown in *S. cerevisiae*, where each RING finger of three RING peroxins has ubiquitin ligase activity as assessed by their self-ubiquitination *in vitro* (30, 36). An *in vitro* ubiquitination assay and genetic analysis show that *S. cerevisiae* Pex12p mediates Pex4p-dependent monoubiquitination of Pex5p (30, 36), whereas Pex2p (30, 36) and Pex10p (37) are implicated to be involved in the Ubc4-dependent polyubiquitination. Self-ubiquitination activity is shown in all three *Arabidopsis thaliana* RING peroxins *in vitro* (38). However, E3 activity of mammalian RING peroxins and their role in Pex5p ubiquitination remain unknown.

Here, we report that RING finger of human Pex10p possesses ubiquitin ligase activity with E2 UbcH5C and that the E3 activity is dramatically augmented by formation of a Pex10p complex with Pex12p. The Pex10p E3 activity is required for peroxisome biogenesis. Moreover, we demonstrate that the Pex10p·Pex12p complex monoubiquitinates Pex5p at multiple lysine residues *in vitro*. We also address two distinct types of Pex5p ubiquitination, cysteine-linked and lysine-linked ubiquitination, and their functional consequences *in vivo*.

MATERIALS AND METHODS

Cell Culture—Wild-type and peroxisome-deficient mutant CHO cells were cultured as described (39, 40). HEK293 cells (41) and fibroblasts from a normal control and PBD patients defective in *PEX12* (42), *PEX10* (43), *PEX2* (44), *PEX1* (45), *PEX6* (46), and *PEX16* (47) were cultured as described.

DNA Constructions—Ubiquitin cDNA was amplified by PCR with reverse transcription products from human skin fibroblasts and with primers Ub-BamFw and Ub-PstRv (supplemental Table S1), as described (43). To construct expression vector coding for tandem HA-tagged ubiquitin (HA_2-Ub) and FLAG-tagged ubiquitin, the BamHI-PstI fragment of the PCR product was inserted together with the NotI (blunted)-BamHI fragment encoding the HA_2 tag from pUcD2Hyg/*HA_2-HsPEX10*[3] or FLAG from pcDNAZeo/*FLAG-HsPEX10* (35), into the BamHI (blunted)-PstI site in pcDNAZeo3.1 (Invitrogen). To construct hexahistidine (His)-tagged UbcH5C, the HindIII-PstI fragment of His-UbcH5C amplified with primers UbcH5C.HisFw and UbcH5C.TGARv and pT7-7/His-UbcH5C (see below) as a template was cloned into the HindIII-PstI site of pcDNAZeo3.1. *HA_2-PEX* expression vectors were constructed by replacing the ubiquitin fragment in pcDNAZeo/*HA_2-Ub* with full-length cDNAs each from *HsPEX10* (43), *RnPEX12* (40), and *RnPEX2* (48). Site-directed mutagenesis in the RING finger of *PEX10* was performed in pUcD2Hyg/*FLAG-HsPEX10* with two-step PCR as described (40).

To express recombinant maltose-binding protein (MBP) fusion proteins, cDNAs encoding wild type and the RING variants of *Hs*Pex10pC (residues 240–326), amplified with primers His-P10C-HA2.Fw and HsP10.TGARv; full-length *Hs*Pex10p with primers HsP10-GST-NFw and BGH.Rv; full-length *Rn*Pex12p with primers RnP12-GST-NFw and BGH.Rv; and RnPex12pC-C304S from pUcD2Hyg/*FLAG-RnPEX12-C304S* (40) were cloned into pMAL-c2X (New England Biolabs). To generate MBP-Pex2pC-HA_2, the PCR products of RnPex2pC (residues 218–305) amplified with primers MBP-Pex2pC.ERFw and MBP-Pex2pC-HA.NheRv were cloned into pMAL-c2X vector by replacing the *PEX10C* fragment in pMAL/*HsPEX10C-HA_2* (35). pMAL-*HA_2* was constructed by self-ligation of pMAL/*HsPEX10C-HA_2* after removing *PEX10* cDNA.

Plasmid pGEX/*EGFP-His-SKL* was constructed by inserting an NcoI (blunt)-SalI fragment from pEGFP/*His-SKL* (49) into the BamHI (blunt)-SalI site in pGEX6P-1 (GE Healthcare). Expression vectors for recombinant His-tagged human E2s, UbcH2A, UbcH2, UbcH3, UbcH4, UbcH5C, UbcH6, UbcH7, and UbcH8 in pT7-7 and UbcH5B in pET-15b were kindly provided by K. Nakayama (Kyushu University). Plasmids for His-*Rn*Pex14p (50) and GST fusion proteins with *Rn*Pex12pC (35), *Hs*Pex13pN (49), *Rn*Pex14p, and *Rn*Pex14pN (residues 1–260) (50) were described previously.

To construct *His-FLAG-ClPEX5L* encoding N-terminally His-FLAG-tagged Pex5p, the BglII-AxyI fragment of the PCR-amplified with primers His-FL-ClP5.Fw and ClP5.AxyRv, and the AxyI-NotI fragment of *ClPEX5L* from pGEX/*ClPEX5L* (14) were cloned together into the BamHI-NotI site of pcDNAZeo/*His-UbcH5C* in which *UbcH5C* had been removed. The epitope tagging is likewise performed for the shorter form of *ClPEX5*, *ClPEX5S*. Plasmids for various KR mutants of Pex5pL were generated by replacing several or all of the 18 lysines in Pex5pL at positions, 19, 28, 52, 83, 170, 205, 210, 218, 273, 293, 315, 360, 392, 449, 465, 499, 520, and 581 with arginine at the DNA level in pcDNAZeo/*His-ClPEX5L-HA* (29) using a PCR-based strategy. These KR mutants of Pex5pL were also expressed as GST fusion proteins by replacing wild-type *PEX5L* cDNA in pGEX/*ClPEX5L* with those for the KR mutants. All mutations and constructions were confirmed by sequencing.

DNA Transfection—DNA transfection to CHO and HEK cells was performed with Lipofectamine (Invitrogen) as

[3] K. Okumoto and Y. Fujiki, unpublished observations.

described (29). Human fibroblasts were transfected by electroporation as described (43). Stable transformants of CHO *pex12* mutant ZP109 (40) expressing FLAG-Pex12p (termed 109/FLP12) and *pex2* Z65 (51) expressing FLAG-Pex2p (65/FLP2) were isolated by transfection of pUcD2Hyg/*FLAG-RnPEX12* (40) and pUcD2Hyg/*FLAG-ClPEX2* (52), respectively, and selection with Hygromycin B (Sigma), as K1/FLP10, a stable transformant of CHO-K1 expressing FLAG-*Hs*Pex10p (35).

Antibodies—We used rabbit antisera to PTS1 peptides (9), Chinese hamster Pex5pS (14), human Pex5pL (residues 1–269),[4] Pex12p (40), Pex10p (29), Pex2p (48), Pex13p (53), Pex14p (54), PMP70 (39), and MBP (New England Biolabs). Mouse monoclonal antibodies to FLAG epitope (M2, Sigma), HA (16B12, Covance), Tom20 (F-10, Santa Cruz Biotechnology, Inc.), ubiquitin (IB3, Molecular and Biological Laboratories, Nagoya, Japan), and α-tubulin (BD Biosciences) and goat antiserum to lactate dehydrogenase (Rockland) were purchased.

Morphological Analysis—Immunostaining for CHO cells and human fibroblasts was performed with primary antibodies and secondary antibodies labeled with Alexa 488 and 568 (Invitrogen) as described (29). Cells were observed under microscopes (LSM510; Carl Zeiss). Images were acquired and analyzed with the LSM image browser (Carl Zeiss).

Immunoprecipitation—Cells were lysed in L-buffer (20 mM Hepes-KOH, pH 7.4, 150 mM NaCl, 1 mM DTT, 1 mM EDTA, 5 μM MG132 (Peptide Institute, Osaka, Japan), and protease inhibitor mixture) containing 1% Triton X-100. For immunoprecipitation of FLAG-RING peroxins, L-buffer containing 1% digitonin (Wako, Osaka, Japan) was used. After centrifugation, the soluble fraction was used for immunoprecipitation with anti-FLAG M2-agarose (Sigma) or anti-HA antibody plus protein G-Sepharose (GE Healthcare) as described (29). Proteins bound to anti-FLAG-agarose were eluted with 100 μg/ml FLAG peptides (Sigma) when required. To more highly purify His-FLAG-Pex5pL, the eluate was denatured in the presence of 1% SDS, diluted with 9 volumes of buffer containing 1% Triton X-100, and then purified with TALON cobalt-chelating resin under a high stringency condition by washing with buffer containing 1 M NaCl. Proteins were eluted with buffer containing 150 mM imidazole and concentrated by precipitation with TCA and subjected to SDS-PAGE and silver staining using a Sil-Best stain kit (Nacalai Tesque, Kyoto, Japan).

Purification of Recombinant Proteins—MBP and GST fusion proteins were purified with amylose resin (New England Biolabs) and glutathione (GSH)-Sepharose beads (GE Healthcare), respectively, as described (35). Purified MBP fusion proteins were eluted by MAL buffer containing 10 mM maltose. Pex5p and its variants were cleaved and isolated from the GST fusion proteins with PreScission protease as described (14). His-tagged proteins were purified by affinity chromatography using TALON cobalt-chelating resin (Invitrogen) as described (35) and eluted with buffer containing 0.2 M imidazole. In the case of His-UbcH5C, eluted His-UbcH5C was dialyzed using a Slide-A-Lyzer cassette (Pierce) in dialysis buffer (40 mM Tris-HCl, pH 7.4, 50 mM NaCl, and 0.1% Triton X-100).

[4] K. Setoguchi and Y. Fujiki, unpublished observations.

Pull-down Assay with GST Fusion Proteins—An *in vitro* binding assay using GST-fused proteins on GSH-Sepharose beads was performed at 4 °C for 2 h in B-buffer (40 mM Hepes-KOH, pH 7.4, 150 mM NaCl, 10% glycerol, 0.1% Triton X-100, 1 mM DTT, protease inhibitors, and 0.2% BSA), as described (29). To prepare Pex5p complexes fully loaded with the interacting proteins, Pex5pL was separately incubated and recovered with GST-EGFP-SKL, GST-Pex14p, and GST-Pex13pN on GSH-Sepharose beads. A ternary complex of Pex5pL with EGFP-SKL and Pex14p was isolated by further incubation of Pex5pL·GST-EGFP-SKL complexes with His-Pex14p. Two types of Pex5pL complexes, His-Pex14p·Pex5pL·GST-EGFP-SKL and Pex5pL·GST-EGFP-SKL, were eluted from GSH-Sepharose by digestion with PreScission protease. Other Pex5pL complexes, Pex5pL·GST-Pex14p and Pex5pL·GST-Pex13pN, bound to GSH-Sepharose beads were eluted with 1 mM GSH and dialyzed as described above. Endogenous Pex5p assessed *in vivo* was likewise recovered with GST-Pex14pN260, encompassing residues 1–260, from cells lysed in L-buffer containing 1% Triton X-100.

In Vitro Ubiquitination Assay—Recombinant His-tagged mouse E1 was kindly provided by H. Yasuda and K. Tanaka. To verify whether RING peroxins exhibit ubiquitin ligase activity, various E2s were first prepared as soluble lysates of *Escherichia coli* BL21(DE3) each expressing His-tagged E2s, including UbcH2A, UbcH2B, UbcH3, UbcH4, UbcH5B, UbcH5C, UbcH6, UbcH7, and UbcH8, in PBS containing 0.1% Triton X-100 and 1 mM PMSF. The ubiquitination assay was performed at 30 °C for 1 h in 25-μl reaction mixtures containing 150 ng of ubiquitin (Sigma), 10 ng of E1, 2.5 μl of lysates of *E. coli* expressing each E2, and 1.5 μg of MBP-RING peroxins in 40 mM Tris-HCl, pH 7.5, 5 mM $MgCl_2$, 2 mM ATP, 2 mM DTT. The reaction was terminated by the addition of SDS-PAGE sample buffer and heating at 95 °C for 5 min. To prepare Cys-ubiquitinated Pex5p, a ubiquitination reaction was performed as described above, except that DTT was omitted.

The ubiquitination assay was likewise performed, except that 1 μg each of MBP-RING fusion proteins, Pex5pL, and Pex5pL-complexes and 250 ng of purified His-UbcH5C as an E2 were used. FLAG-HsPex10p immunopurified from K1/FLP10 cells was also used as an E3. Wild-type ubiquitin and its mutants, K48R, K63R, and K0 (Boston Biochem), were used where indicated.

In Vitro Import and Export Assays of Pex5p—Assays for *in vitro* import and export of Pex5p were performed as described (17). Briefly, ^{35}S-labeled Pex5pL and its variants were synthesized *in vitro* by a coupled transcription and translation of respective cDNAs. Import reaction was performed at 26 °C for 60 min with ^{35}S-Pex5pL and postnuclear supernatant (PNS) from a *PEX5*-deficient CHO mutant ZP105 (9) in the absence of ATP for 60 min at 26 °C. Imported ^{35}S-Pex5pL was verified by its resistance to 5 μg/ml Proteinase K digestion.

^{35}S-Pex5pL export from the organellar fraction after the import reaction was assessed in the presence of the cytosolic fraction of ZP105, ATP, and the ATP-regenerating system (17). ^{35}S-Pex5pL was detected by a FujiX FLA5000 Autoimaging analyzer (Fujifilm) and quantified with Image Gauge software (Fujifilm).

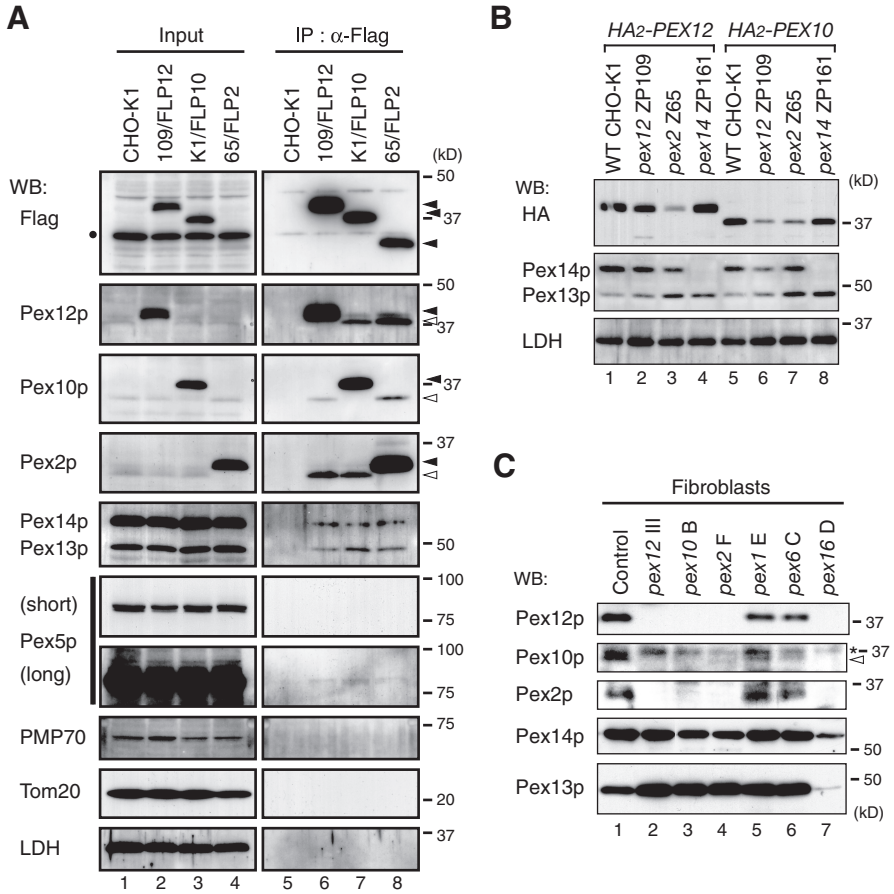

FIGURE 1. **RING peroxins form a complex.** *A*, immunoprecipitation of RING peroxins. CHO-K1, FLAG-Pex12p-expressing *pex12* ZP109 (109/FLP12), CHO-K1 stably expressing FLAG-Pex10p (K1/FLP10), and *pex2* Z65 expressing FLAG-Pex2p (65/FLP2) (1.5×10^7 cells each) were solubilized and subjected to immunoprecipitation (*IP*) with anti-FLAG-antibody conjugated to agarose. Immunoprecipitates eluted with FLAG peptides were analyzed by SDS-PAGE and immunoblotting (*WB*) with the antibodies indicated on the *left*. *Input*, 5% cell lysates used for immunoprecipitation. *Solid* and *open arrowheads* indicate FLAG-tagged and endogenous RING peroxins, respectively. *, nonspecific band. *B*, RING peroxins in peroxisome-deficient CHO mutants. Plasmids each encoding HA_2-*PEX12* and HA_2-*PEX10* were transfected to CHO-K1, *pex12* ZP109, *pex2* Z65, and *pex14* ZP161. At 36 h after the transfection, cells were lysed and analyzed by SDS-PAGE and immunoblotting with the antibodies indicated on the *left*. *C*, stability of endogenous RING peroxins in peroxisome-deficient fibroblasts from PBD patients. Cell lysates from a normal control (control) and PBD patients each with deficiency of *PEX12*, *PEX10*, *PEX2*, *PEX1*, *PEX6*, and *PEX16* were assessed by immunoblotting with the antibodies indicated on the *left*. The *arrowhead* and *asterisk* indicate endogenous Pex10p and a nonspecific band, respectively.

Proteolytic Digestion of Pex5p—One μl of the reticulocyte lysates containing *in vitro* synthesized ^{35}S-Pex5pL variants was incubated on ice for 15 min in 50 μl of buffer (50 mM Tris-HCl, pH 7.4, 150 mM NaCl, 1 mM EDTA, 1 mM DTT) containing 0.2 μg/ml Proteinase K. The reaction was terminated by adding 0.5 mg/ml PMSF and analyzed by SDS-PAGE and autoradiography as described above.

Other Methods—Subcellular fractionation of various cultured cells was performed in homogenization buffer (5 mM Hepes-KOH, pH 7.4, 0.25 M sucrose) containing protease inhibitor mixture (Roche Applied Science), 5 μM MG132, and 5 mM *N*-ethylmaleimide, as described (29). Western blot analysis was performed using various primary antibodies described above and horseradish peroxidase-conjugated secondary antibodies to mouse or rabbit IgG (GE Healthcare), or goat IgG (Cappel) with an ECL reagent (GE Healthcare).

RESULTS

Three RING Peroxins Interact with Each Other—We established three stable CHO cell lines, each expressing N-terminally FLAG-tagged RING peroxins: wild-type CHO-K1 expressing FLAG-Pex10p, termed K1/FLP10; *pex12* mutant ZP109 expressing FLAG-Pex12p, 109/FLP12; and *pex2* Z65 expressing FLAG-Pex2p, Z65/FLP2. In these cell lines, three FLAG-RING peroxins localized to peroxisomes, and morphologically and biochemically normal peroxisomes were discernible (data not shown). Upon immunoprecipitation of FLAG-Pex10p from K1/FLP10 cells lysed with 1% digitonin, endogenous Pex2p and Pex12p were coimmunoprecipitated (Fig. 1*A*, *lanes 3* and *7*), consistent with our earlier report (35). Likewise, in the immunoprecipitates of FLAG-Pex12p and FLAG-Pex2p, the two endogenous RING peroxins were recovered (Fig. 1*A*, *lanes 2*, *4*, *6*, and *8*). Together, we interpreted these findings to mean that three RING peroxins interact with each other. Pex14p and Pex13p, components of the matrix protein import machinery, were detected at a lower level in the immunoprecipitates of the FLAG-RING peroxins (Fig. 1*A*, *lanes 6–8*). Moreover, a smaller amount of Pex5p was also detectable. Specificity of the interactions between RING peroxins and other peroxins was confirmed by immunoblotting of the 70-kDa peroxisomal membrane protein and cytosolic lactate dehydrogenase (Fig. 1*A*).

However, Pex14p, Pex13p, and Pex5p were not detectable in the FLAG-Pex10p immunoprecipitates from K1/FLP10 cells

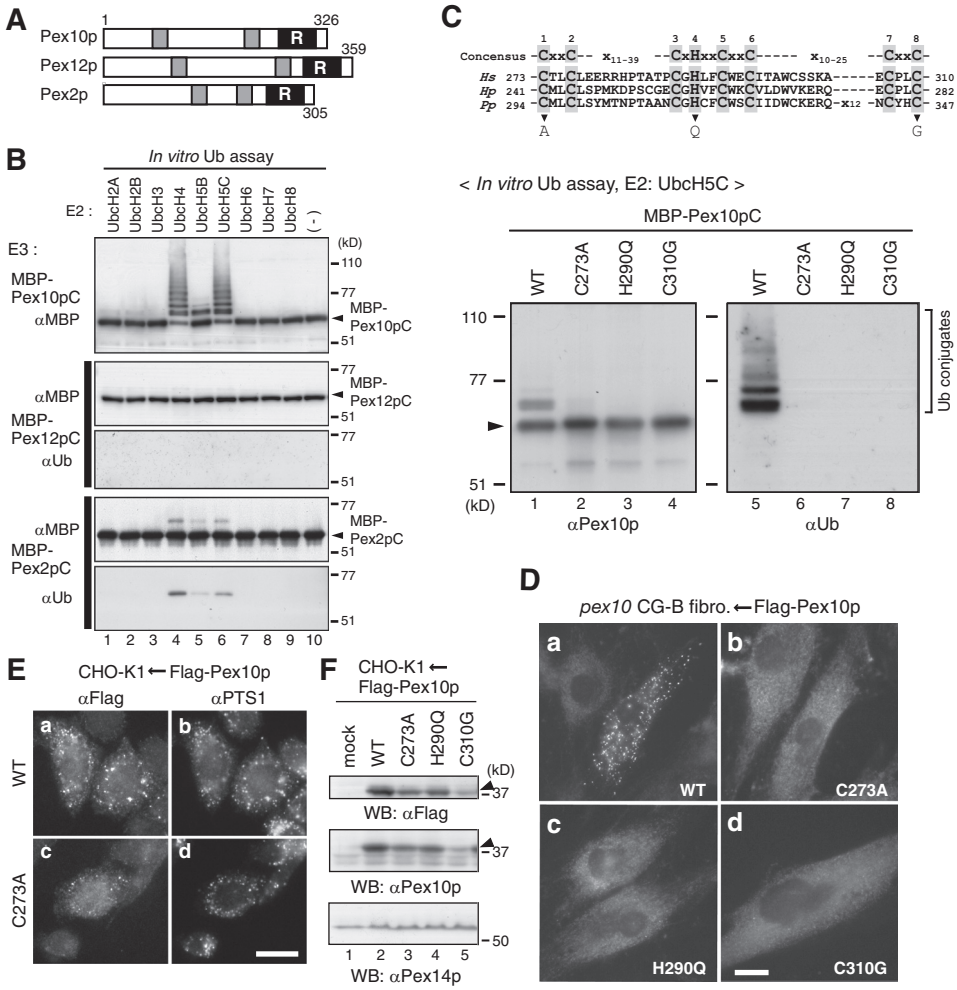

FIGURE 2. **RING finger of Pex10p shows self-ubiquitinating activity *in vitro* and is required for its complementing activity of *pex10* fibroblasts *in vivo*.** *A*, schematic diagram of domain structure of RING peroxins. *Gray boxes*, transmembrane domains; *black boxes labeled R*, RING finger motifs. *B*, modification of MBP-Pex10pC *in vitro*. An *in vitro* ubiquitination assay was performed using nine E2 enzymes, each with MBP-Pex10pC (*top*), MBP-Pex12pC (*middle*), and MBP-Pex2pC (*bottom*) as described under "Materials and Methods." Reaction mixtures were assessed by immunoblotting with anti-MBP antibody. *C*, self-ubiquitination of MBP-Pex10pC depends on its RING finger. *Top*, alignment of amino acid sequences of the RING finger in Pex10p from *HsPEX10* (*Homo sapiens*), *HpPEX10* (*Hansenula polymorpha*), and *PpPEX10* (*P. pastoris*). The eight amino acid residues, C_3HC_4, conserved in the RING finger are *shaded*; mutations used in this study are indicated *below*. *Bottom*, an *in vitro* ubiquitination assay was performed with wild-type and mutant MBP-Pex10pC in the presence of E2 UbcH5C. The reaction mixtures were verified by immunoblotting with antibodies to Pex10p (*left*) and Ub (*right*). *Solid arrowhead*, non-modified MBP-Pex10pC. *D*, complementing activity of Pex10p RING mutants. Fibroblasts from a *PEX10*-defective PBD patient (PBDB-01) were transfected with plasmids encoding FLAG-Pex10p variants. At 48 h after the transfection, cells were immunostained with anti-PTS1 antibody. *Bar*, 10 μm. *E*, localization of Pex10p RING mutants. CHO-K1 cells were transfected with plasmids encoding wild-type FLAG-Pex10p and the RING mutant C273A. At 24 h post-transfection, cells were immunostained with antibodies to FLAG (*a* and *c*) and PTS1 (*b* and *d*). *Bar*, 10 μm. *F*, stability of Pex10p RING mutants. CHO-K1 cells were transfected as in *E* and then lysed and analyzed by immunoblotting (*WB*) with the antibodies indicated at the *bottom*. *Arrowheads*, exogenously expressed FLAG-Pex10p variants.

when lysed with 1% Triton X-100 (data not shown), consistent with our earlier report (35), suggesting that three RING peroxins formed a trimeric core complex involving Pex14p, Pex13p, and Pex5p as the subcomplex. Furthermore, exogenously expressed HA_2-Pex10p was apparently decreased in *pex12* mutant ZP109 and *pex2* Z65 relative that in CHO-K1 and *pex14* ZP161 (Fig. 1*B*, *lanes 5–8*). HA_2-Pex12p was also unstable in Z65, but not in ZP109, CHO-K1, and ZP161 (Fig. 1*B*, *lanes 1–4*), where HA2-Pex12p complemented peroxisomal deficiency in ZP109 (*lane 2*). Similarly, each endogenous RING peroxin was hardly detectable in fibroblasts from patients with PBD deficient in two other RING peroxins and membrane assembly-defective *pex16* complementation groups (Fig. 1*C*, *lanes 2–4* and *7*). In contrast, lower levels of three RING peroxins were detected in fibroblasts from *pex1* and *pex6* PBD patients (Fig. 1*C*, *lanes 1*, *5*, and *6*). These results suggested that the deficiency of one RING peroxin affected the stability of two other RING peroxins, as observed in yeast (30, 55).

RING Finger of Pex10p Is Required for the Self-ubiquitination and the Complementing Activity—RING fingers of three RING peroxins are indispensable for the complementing activity of the impaired peroxisome biogenesis in respective *pex* mutant cells, but the molecular mechanisms underlying such activity remain unknown. Recent findings that RING fingers in many proteins possess E3 activity (31) prompted us to verify E3 activity in the RING fingers of mammalian RING peroxins (Fig. 2*A*). In an *in vitro* ubiquitination assay using respective recombinant MBP-RING fusion proteins with ATP, ubiquitin, E1, and various E2s, MBP-Pex10pC gave rise to high molecular mass ladder bands in the presence of UbcH4 and UbcH5C (Fig. 2*B*, *top*,

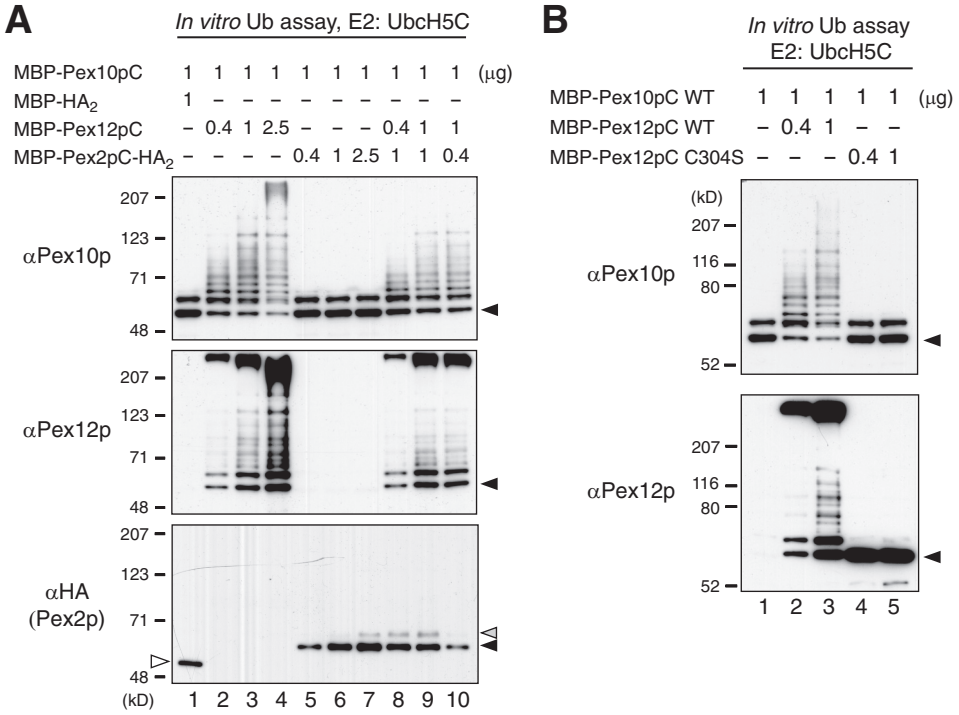

FIGURE 3. **RING finger of Pex12p enhances ubiquitin ligase activity of Pex10pC.** *A*, *in vitro* ubiquitination assay was performed with MBP-Pex10pC, MBP-Pex12pC, MBP-Pex2pC-HA_2, and MBP-HA_2 as indicated at the *top* in the presence of E2, UbcH5C. The reaction mixtures were analyzed by immunoblotting with antibodies to Pex10p, Pex12p, and HA. *Solid*, *open*, and *shaded arrowheads*, respective authentic MBP-RING peroxins, MBP-HA_2, and the self-ubiquitinated form of MBP-Pex2pC-HA_2, respectively. *B*, ubiquitination assays were likewise performed as in *A* with MBP-Pex10pC, MBP-Pex12pC, and MBP-Pex12pC-C304S (a RING mutant of Pex12pC), as indicated.

lanes 4 and *6*) and, to a lesser extent, with UbcH5B (*lane 5*). Immunoblotting with anti-ubiquitin antibody confirmed that MBP-Pex10pC was modified with ubiquitin (Fig. 2*C*, *bottom*, *lanes 1* and *5*). However, no ubiquitin-conjugated bands were discernible with several RING finger mutants of Pex10pC, including C273A with the first Cys mutated to Ala, H290Q identified in a *pex10* PBD patient (56), and C310G, representing the eighth Cys substituted to Gly (Fig. 2*C*), thereby confirming the RING-dependent self-ubiquitination activity of MBP-Pex10pC *in vitro*, as shown in the RING domain of *S. cerevisiae* Pex10p (19, 30). MBP-Pex2pC showed a small amount of a single band with ubiquitin modification in the presence of UbcH4 and UbcH5C (Fig. 2*B*, *two bottom panels*, *lanes 4* and *6*) and a lesser amount with UbcH5B (*lane 5*). This result strongly suggested that MBP-Pex2pC has self-ubiquitination activity *in vitro*, although the activity is much lower than MBP-Pex10pC. MBP-Pex12pC showed no such self-ubiquitination activity with each of the E2s examined (Fig. 2*B*, *two middle panels*), in contrast to the E3 activity of the RING finger of Pex12p in *S. cerevisiae* (30) and *A. thaliana* (38). No self-ubiquitination of each mammalian RING finger was detectable in the *in vitro* ubiquitination reaction with *S. cerevisiae* Pex4p as an E2 (data not shown).

Next, we examined the peroxisome-restoring activity of FLAG-Pex10p RING variants by transfection of their cDNAs to fibroblasts from a *pex10* PBD patient of complementation group B (PBDB-01) expressing Pex10p truncated in the RING finger (43). The impaired matrix protein import was complemented by wild-type *FLAG-PEX10* expression as assessed by immunostaining with anti-PTS1 antibody (Fig. 2*D*, *a*), as in our earlier report (43). In contrast, none of the RING mutants, C273A, H290Q, and C310G, restored PTS1 protein import (Fig. 2*D*, *b–d*). Like the wild-type (Fig. 2*E*, *a* and *b*), FLAG-Pex10p RING mutants C273A (*c* and *d*), H290Q, and C310G (data not shown) were localized to punctate structures, peroxisomes, as verified by co-localization with PTS1 proteins in CHO-K1 cells, but apparently at a lower expression level than the wild-type (Fig. 2*F*, *lanes 1–5*), indicative of the peroxisomal localization of Pex10p RING mutants. In conclusion, the RING finger of Pex10p is not essential for localization of Pex10p to peroxisomes but is required for peroxisome-restoring activity and E3 activity of Pex10p.

Pex12p RING Finger Enhances Pex10p E3 Activity—To investigate whether Pex10p RING interacting partners, Pex2p and Pex12p, show any effects on the E3 activity of the Pex10p RING, we performed the *in vitro* ubiquitination assay using MBP-Pex10pC in the presence of MBP-Pex2pC and MBP-Pex12pC. The self-ubiquitination activity of MBP-Pex10pC was significantly elevated by incubation with MBP-Pex12pC in an MBP-Pex12pC-dependent manner, as compared with the reaction with a control MBP-HA_2 (Fig. 3*A*, *top*, *lanes 1–4*). Such augmentation of MBP-Pex10pC ubiquitination was not detectable with MBP-Pex2pC-HA_2 (*lanes 5–7*). MBP-Pex12pC was also highly ubiquitinated in these assays (Fig. 3*A*, *middle*, *lanes 1–7*). A RING mutant, MBP-Pex12pC-C304S, does not interact with Pex10p RING (35). MBP-Pex12pC-C304S showed neither enhancement of the self-ubiquitination activity of MBP-Pex10pC nor its ubiquitination (Fig. 3*B*), thereby suggesting that the binding of MBP-Pex10pC to Pex12p-RING was a prerequisite for augmenting its E3 activity. On the other hand, in

the presence of both MBP-Pex12pC and MBP-Pex2pC-HA_2 at a different ratio, MBP-Pex12pC-dependent augmentation in the level of ubiquitinated MBP-Pex10pC and MBP-Pex12pC was similar to that of MBP-Pex10pC only with MBP-Pex12pC (Fig. 3*A*, *lanes 8–10*), hence suggesting that MBP-Pex2pC-HA_2 did not affect the ubiquitination of MBP-Pex10pC and MBP-Pex12pC. MBP-Pex10pC and MBP-Pex12pC showed a slightly additive effect in ubiquitination of MBP-Pex2pC-HA_2 (Fig. 3*A*, *bottom*, *lanes 7–9*, *shaded arrowhead*), possessing weak self-ubiquitination activity with the same E2s as for MBP-Pex2pC (data not shown), implying that the MBP-Pex10pC and MBP-Pex12pC complex enhanced the self-ubiquitination activity of MBP-Pex2pC-HA_2 and ubiquitinated MBP-Pex2pC-HA_2 as a substrate. Neither E3 activity nor an additive effect was observed in the reaction with a set of MBP-Pex12pC and MBP-Pex2pC-HA_2 (data not shown). Taken together, these results indicated that the Pex12p RING finger functioned as an activator of the E3 ligase Pex10p.

Pex10p·Pex12p Complex Ubiquitinates PTS1 Receptor Pex5p—Monoubiquitination of the conserved cysteine residue at the N-terminal region of the PTS1 receptor Pex5p is shown to be a key regulation of its shuttling between the cytosol and peroxisomes (20, 27, 29, 57). Although RING peroxin-dependent ubiquitination of Pex5p has been shown in yeast (30, 37), a role of RING peroxin in Pex5p ubiquitination remains unknown in mammals. Therefore, we investigated whether Pex5p is a substrate of Pex10p RING E3. In an *in vitro* ubiquitination reaction, Pex5pL was detected in several slower migrating bands, presumably representing ubiquitinated Pex5pL, when incubated with wild-type MBP-Pex10pC plus MBP-Pex12pC (Fig. 4*A*, *lane 4*), not with MBP-Pex10pC or MBP-Pex12pC alone (*lanes 1* and *2*). E3 activity of MBP-Pex10pC was not altered in the absence or presence of Pex5pL as assessed by ubiquitination of MBP-Pex10pC and MBP-Pex12pC (Fig. 4*A*, *lanes 3* and *4*). Furthermore, after the *in vitro* ubiquitination assay, ubiquitin-conjugated Pex5pL-FLAG was detected only in the immunoprecipitate of wild-type Pex5pL-FLAG, not in that of the K-less Pex5pL-FLAG in which all Lys residues had been replaced with Arg (data not shown), hence confirming the specific ubiquitination of Pex5pL. In contrast, such higher mass bands of Pex5pL were not discernible when the assay was performed with MBP-Pex10pC-WT plus a Pex12pC RING mutant, MBP-Pex12pC-C304S, defective in augmenting Pex10pC-WT ubiquitination (Fig. 4*A*, *lanes 5* and *6*).

Furthermore, the *in vitro* ubiquitination assay was likewise performed using an E3 FLAG-Pex10p that had been immunoprecipitated from K1/FLP10 cells. FLAG-Pex10p immunocomplex, apparently with a low level of endogenous Pex12p, ubiquitinated MBP-Pex12pC, but not MBP-Pex12pC-C304S, where the self-ubiquitinated forms of FLAG-Pex10p were barely detectable (Fig. 4*B*, *lanes 1–4*). Accordingly, the full-length Pex10p also exerted the ubiquitin ligase activity *in vitro* as Pex10pC did. Moreover, Pex5p was detected as several bands with higher masses, presumably ubiquitinated Pex5pL, as well as the authentic size, upon incubation with the FLAG-Pex10p immunocomplex (Fig. 4*B*, *lane 5*). The extent of Pex5pL ubiquitination was not altered by the addition of wild-type and C304S-type MBP-Pex12pC (Fig. 4*B*, *lanes 6* and *7*). Apparent ubiquitination of Pex5pL in the absence of MBP-Pex12pC can be explained by the presence of endogenous Pex12p in the FLAG-Pex10p immunoprecipitates as a complex (see Fig. 4*B*, *endo*. *Pex12p panel*). Essentially the same results were obtained with Pex5pS in place of Pex5pL (data not shown).

Next, we verified Pex5pL ubiquitination by an *in vitro* ubiquitination assay using full-length Pex10p and Pex12p as an E3 complex. MBP-Pex10pFull, not MBP-Pex12pFull, showed a higher mass band, indicative of self-ubiquitination activity of Pex10pFull (Fig. 4*C*, *lanes 1* and *2*), although apparently lower than MBP-Pex10pC (Fig. 3*A*, *lane 1*). The ubiquitination of MBP-Pex10pFull was moderately augmented with the addition of MBP-Pex12pFull, where MBP-Pex12pFull was hardly ubiquitinated (Fig. 4*C*, *lane 3*), contrary to MBP-Pex12pC with MBP-Pex10pC (Fig. 3). Pex5pL was ubiquitin-modified upon incubation with a mixture of MBP-Pex10pFull and MBP-Pex12pFull, but not with MBP-Pex10pFull or MBP-Pex12pFull, in a manner dependent on E1 and E2 (Fig. 4*C*, *lanes 4–9*).

To determine the mode of Pex5p ubiquitination, we performed an *in vitro* ubiquitination assay with ubiquitin mutants, K48R and K63R, giving rise to abrogation of Lys^{48}-, Lys^{63}-linked ubiquitin chain elongation, and K0, resulting in no elongation. No difference was discernible between the wild type and mutants in higher mass bands, the ubiquitinated Pex5pL (Fig. 4*D*, *top*, *lanes 5–8*), strongly suggesting that Pex5pL was monoubiquitinated at multiple lysine residues by the Pex10p·Pex12p complex. Such a multimonoubiquitination was also evident in the self-ubiquitination of Pex10p (Fig. 4*D*, *middle*, *lanes 1–8*).

In vitro ubiquitination assays described above demonstrated the covalent ubiquitination of Pex5p via lysine residues. Monoubiquitination was recently identified in the conserved cysteine residue of mammalian Pex5p (27–29, 58). As a step to identifying an E3 for Cys-ubiquitination of Pex5p, we examined whether RING peroxins catalyze the DTT-sensitive ubiquitination of Pex5p *in vitro*. As shown in Fig. 4*A*, MBP-Pex10pC plus MBP-Pex12pC, not MBP-Pex10pC or MBP-Pex12pC alone, exhibited ubiquitination of wild-type Pex5pL, but no difference was discernible in the slowly migrating bands in the absence or presence of DTT (Fig. 4*E*, *lanes 1–4* and *6–9*). MBP-Pex2pC showed no effect on ubiquitination of wild-type Pex5pL by the Pex10pC·Pex12pC E3 complex under both conditions (Fig. 4*E*, *lanes 5*, *10*, *15*, and *20*), where no E3 ligase activity for Pex5pL was detectable with MBP-Pex2pC (*lanes 11–14* and *16–19*). Pex5pL-C11A, a Pex5pL variant with a mutation of the ubiquitinated Cys^{11} residue to Ala (29), was ubiquitinated in the presence of MBP-Pex10pC and MBP-Pex12pC, like wild-type Pex5pL, only in a DTT-resistant manner (Fig. 4*E*, *lanes 4* and *9*). Taken together, we conclude that Pex5p is a substrate of the ubiquitin ligase Pex10p·Pex12p complex via lysine residues *in vitro*. However, we could not exclude the possibility that the Pex10p·Pex12p RING complex requires other potential E2 enzyme to catalyze Cys-ubiquitination of Pex5p.

Pex14p, but Not Pex13p, Interferes with Pex5p Ubiquitination—To investigate whether Pex5p ubiquitination shows any effects on PTS1 protein import, Pex5p proteins were fully loaded with the interacting proteins and assayed as substrates for the *in vitro* ubiquitination reaction. As compared with Pex5pL, the ubiquitination of Pex5pL in a complex with Pex14p was signif-

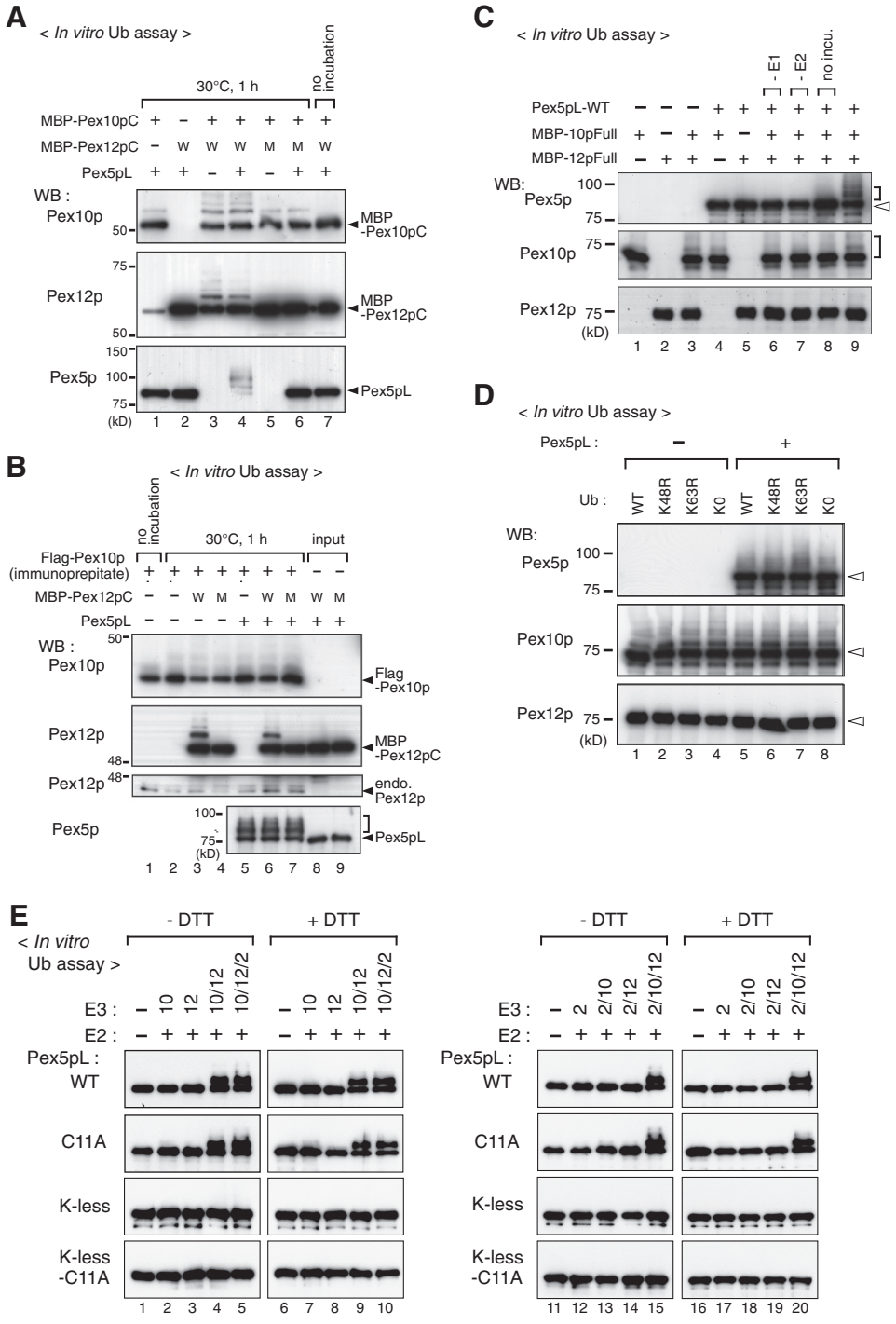

FIGURE 4. **Pex5p is a potential substrate of Pex10p·Pex12p ubiquitin ligase complex.** *A*, *in vitro* ubiquitination of Pex5p. Wild-type MBP-Pex10pC, wild type (*W*) or C304S mutant (*M*) of MBP-Pex12pC, and Pex5pL were assessed by an *in vitro* ubiquitination assay as in Fig. 2*C*. *B*, K1/FLP10-derived FLAG-Pex10p ubiquitinates Pex5p and Pex12p. The *in vitro* ubiquitination assay was performed as in *A*, using wild type (*W*) or C304S mutant (*M*) of MBP-Pex12pC, Pex5pL, and an E3, FLAG-Pex10p immunoprecipitated from K1/FLP10 cells. Ubiquitinated Pex5p bands are designated with a *bracket*. *C*, *in vitro* ubiquitination assay was performed with MBP-fused full-length Pex10p (MBP-10pFull) and Pex12p (MBP-12pFull), in the absence (−) or presence (+) of Pex5pL. *Arrowhead* and *bracket*, unmodified and ubiquitinated Pex5pL, respectively. *D*, *in vitro* ubiquitination assay was performed as in *lane 9* in *C*, except for using wild-type ubiquitin (*WT*) or its mutants, K48R, K63R, and K0. *Arrowheads*, unmodified Pex5pL (*top*), MBP-Pex10pFull (*middle*), and MBP-Pex12pFull (*bottom*). Note that apparently monoubiquitinated Pex5p and Pex10p were discernible in all types of K-mutants of ubiquitin. *E*, an *in vitro* ubiquitination assay was performed as in *A* using MBP-Pex10pC, MBP-Pex12pC, MBP-Pex2pC, and Pex5pL variants, as indicated, where DTT was omitted from the reaction mixture. The reaction was terminated by incubation in Laemmli SDS-PAGE sample buffer in the absence of DTT at 50 °C (−) for 10 min (*lanes 1–5* and *11–15*) or presence of 0.1 M DTT at 100 °C (+) for 5 min (*lanes 6–10* and *16–20*). Note that DTT-sensitive ubiquitin modification of Pex5pL was hardly detectable with any single RING peroxin or any combination of them. *WB*, Western blot.

icantly inhibited and completely abrogated when mixed with Pex14p and PTS1 protein (Fig. 5*A*, *lanes 2*, *6*, and *8*). Pex5pL loaded with PTS1 protein was less efficiently ubiquitinated (*lane 4*). In contrast, Pex5pL bound to Pex13pN was highly ubiquitinated (*lane 10*). These results implied that the ubiquitination of Pex5pL by the Pex10p·Pex12p complex is differen-

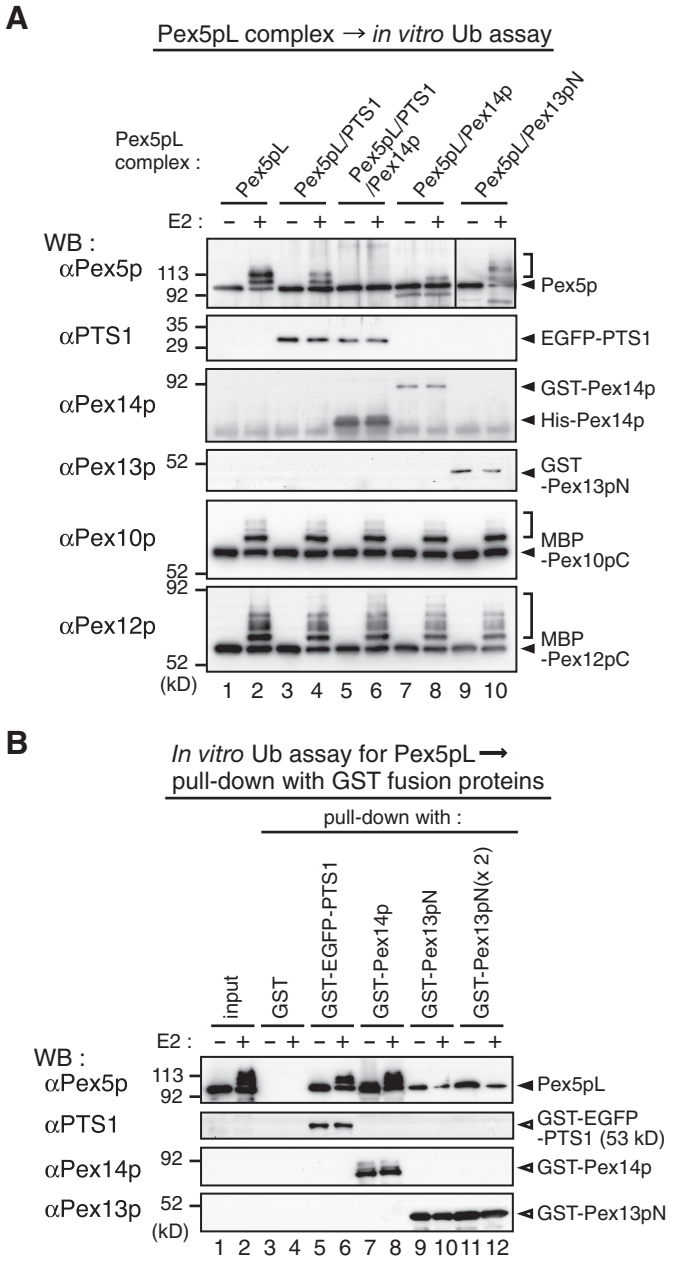

FIGURE 5. **Pex14p interferes with ubiquitination of Pex5p.** *A*, *in vitro* ubiquitination of Pex5p in the form of complexes with its interacting proteins. Pex5pL fully loaded with EGFP-PTS1, Pex14p, Pex13p, or EGFP-PTS1 plus His-Pex14p was prepared as described under "Materials and Methods." The *in vitro* ubiquitination assay was performed as indicated at the *top*, in the absence (−) or presence (+) of E2. *B*, interaction between ubiquitinated Pex5p and Pex5p-binding proteins. *In vitro* ubiquitination of Pex5pL was performed as in *A*, in the absence (−) or presence (+) of E2. The reaction mixtures were subjected to pull-down assays using GSH-Sepharose separately conjugated with the respective proteins as indicated at the *top*. Equal aliquots of respective fractions were analyzed as in *A*. *WB*, Western blot.

tially regulated by its complex formation with proteins, including the cargoes and the constituent peroxins in the peroxisome import machinery. No ubiquitin modification was observed in PTS1 protein, Pex14p, and Pex13pN in the complexes with Pex5p (Fig. 5*A*, *lanes 4*, *6*, *8*, and *10*), strongly suggesting that ubiquitin ligase activity of the Pex10p·Pex12p complex is highly specific to Pex5p. Next, we assessed whether the ubiquitination of Pex5p alters the affinity to the binding partners. Pex5p was initially ubiquitinated with the Pex10p·Pex12p complex *in vitro*, and the reaction mixtures were then subjected to pull-down assays using Pex5p-interacting proteins fused with GST (Fig. 5*B*). Both the ubiquitinated and unmodified forms of Pex5pL were detected nearly at the same level in the bound fractions to GST-EGFP-PTS1 and GST-Pex14p, but not to GST (Fig. 5*B*, *lanes 1–8*), thereby indicating that the ubiquitination did not alter the interaction of Pex5pL with PTS1 protein and Pex14p. In contrast, only non-ubiquitinated Pex5pL was detectable in the fraction bound to GST-Pex13pN (*lanes 9* and *10*). Together with the results described above (Fig. 5*A*), we interpreted these findings to mean that the Pex10p·Pex12p complex efficiently ubiquitinated Pex5pL in the complex with Pex13p, not Pex14p, and the ubiquitinated Pex5pL was dissociated from Pex13p.

In Vivo Ubiquitination of Pex5p via Cysteine and Lysine Residues—In mammalian cells, two types of modified Pex5p were identified: a DTT-sensitive form with monoubiquitination at a conserved cysteine residue, which is associated with peroxisomes in rat liver (28), rat hepatoma Fao cells (29, 58), and HeLa cells (58) and a DTT-insensitive form with unknown modification in the cytosol in Fao and HeLa cells (29, 58). We performed subcellular fractionation of HEK293 cells in homogenization buffer containing *N*-ethylmaleimide to inhibit deubiquitination of the ubiquitin-modified proteins (59). In immunoblot analysis of Pex5p, Pex5p in the PNS fraction was mostly recovered in the cytosolic fraction, and the remainder (about 15%) was in the organellar fraction in the absence and presence of DTT (Fig. 6*A*, *open arrowhead*; note that organellar fractions were loaded as 6-fold aliquots of PNS and cytosolic fractions), as in other mammalian cells (14, 29). A Pex5p-related band with slower migration was similarly discernible in the cytosolic and organellar fractions in a DTT-resistant manner (Fig. 6*A*, *shaded arrowhead*), suggesting a covalent modification of Pex5p. Furthermore, an additional band with a slightly lower migration adjacent to the DTT-resistant Pex5p-related band was detected only in the organellar fraction in the absence of DTT (Fig. 6*A*, *lane 3*, *solid arrowhead*), which then disappeared upon treatment with DTT (*lane 6*). During cell fractionation, *N*-ethylmaleimide was essentially required to detect the DTT-sensitive modification of Pex5p (Fig. 6*A*, *lanes 7* and *8*). These DTT-resistant and -sensitive modifications of Pex5p were likewise detected in mouse embryonic fibroblasts and mouse leukemic monocyte macrophage cell line RAW264.7 (data not shown). The DTT-sensitive modification most likely corresponds to a monoubiquitination at the Cys^{11} residue of Pex5p in Fao cells (29). Treatment with MG132, a proteasome inhibitor, gave rise to an additional DTT-resistant band of Pex5p with slower migration than Lys-ubiquitinated Pex5p (Fig. 6*A*, *lane 11*, *solid dot*), where neither intracellular localization nor protein stability of Pex5p was altered (*lanes 9–12*). Together, these results strongly suggested two distinct types of modification of Pex5p in mammalian cells.

To assess the DTT-resistant modification of Pex5p *in vivo*, endogenous Pex5p in the lysates of HEK293 cells was pulled down with GST-Pex14p and analyzed under the reducing condition (Fig. 6*B*). Immunoblotting with anti-Pex5p antibody showed that GST-Pex14p, not GST, recovered both endoge-

nous Pex5p as doublet bands of ~80 kDa, most likely containing the short and long isoforms of Pex5p (9) (Fig. 6*B*, *top*, *lanes 1*, *3*, and *6*, *open arrowhead*), and a slower migrating 90-kDa band of covalently modified Pex5p (*solid arrowhead*). When HA_2-Ub was expressed in HEK293 cells, an HA-positive band with corresponding migration to the 90-kDa Pex5p-related band was specifically recovered with GST-Pex14p (Fig. 6*B*, *middle panel*, *lane 4*, *solid arrowhead*), suggesting that the 90-kDa band was Pex5p covalently conjugated with HA_2-Ub. In HEK cells expressing HA_2-Ub, an additional mobility shift of the more slowly migrating forms of endogenous Pex5p was hardly detectable in the cell lysates (Fig. 6*B*, *lanes 1* and *2*) and both cytosolic and organellar fractions (data not shown). We interpreted these data to mean that a portion of endogenous Pex5p was covalently ubiquitinated, but the exogenously expressed HA_2-Ub was much less efficiently utilized in the Pex5p ubiquitination. Taken together, these data strongly suggested that endogenous Pex5p was ubiquitinated at the lysine residue mainly in the cytosol, in addition to the Cys^{11} ubiquitination in peroxisomes (27, 29).

We next verified whether Pex5p is ubiquitinated in peroxisome-deficient CHO cell mutants. In wild-type CHO-K1 cells,

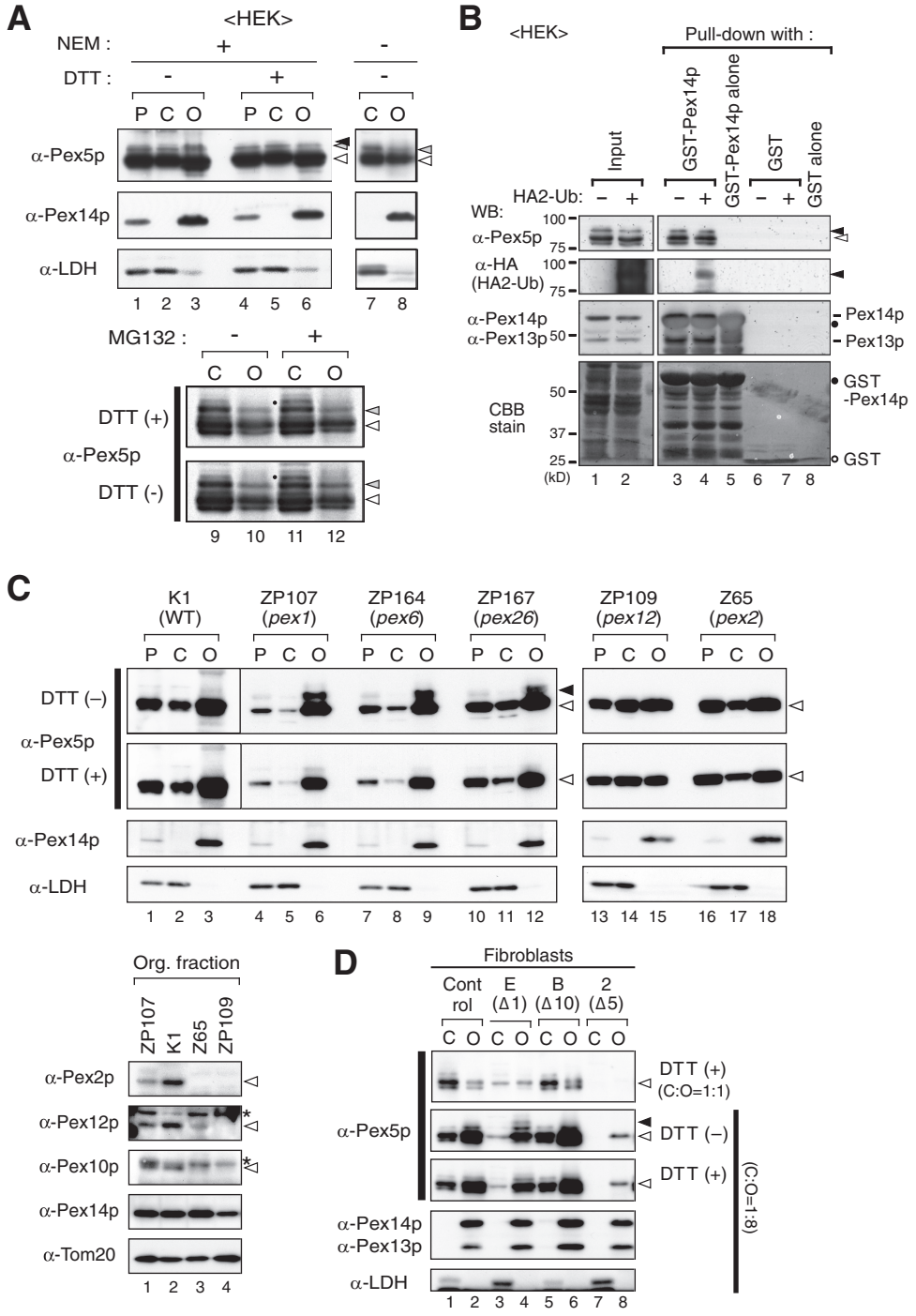

most of the unmodified Pex5p was recovered in the cytosolic fraction, and about 10% was in the organellar fraction (Fig. 6*C*, *top panels*, *lanes 1–3*), as in HEK cells (Fig. 6*A*). A small amount of DTT-sensitive Pex5p was also detectable in the peroxisomal fraction (Fig. 6*C*, *top panels*, *lanes 1–3*, *solid arrowhead*). Covalent ubiquitination of Pex5p in CHO-K1 cells was apparently much less than in HEK cells (Fig. 6*A*) and HeLa cells (58). It was noteworthy that Pex5p with DTT-sensitive modification, most likely Cys-ubiquitinated Pex5p, appeared to be accumulated in the organellar fractions in Pex5p export-deficient CHO mutants *pex1* ZP107, *pex6* ZP164, and *pex26* ZP167 (17) (Fig. 6*C*, *top*, *lanes 6*, *9*, and *12*, *solid arrowhead*), where the amount of unmodified Pex5p in the PNS and cytosolic fractions was significantly reduced in ZP107 and ZP164 (*lanes 4–9*, *open arrowhead*), as reported in *PEX1*- and *PEX6*-deficient fibroblasts (33). In *PEX1*-deficient fibroblasts, similar DTT-sensitive modification of Pex5p accumulated in the organellar fraction and lower stability of unmodified Pex5p in the cytosolic fraction were observed (Fig. 6*D*, *lanes 3* and *4*), in contrast to normal fibroblasts (*lanes 1* and *2*), suggesting that an export-competent, Cys-ubiquitinated form of Pex5p accumulated in peroxisomes in Pex5p export-defective cells. On the other hand, no DTT-sensitive modification of Pex5p was discernible in the respective organellar fractions in RING peroxin-deficient CHO mutants, *pex12* ZP109 and *pex2* Z65 (Fig. 6*C*, *top panels*, *lanes 15* and *18*), and in *PEX10*-deficient PBD fibroblasts (Fig. 6*D*, *lane 6*), despite relatively higher accumulation of unmodified Pex5p in these organellar fractions, as shown in fibroblasts from PBD patients defective in any of three RING peroxins (33). Pex5p in the cytosolic fraction was decreased in *pex12* ZP109 and *pex2* Z65 (Fig. 6*C*, *top panels*, *lanes 14* and *17*) and in *PEX10*-deficient PBD fibroblasts (Fig. 6*D*, *lane 5*), which suggests that the Pex1p·Pex6p AAA complex plays a protective role against proteasomal degradation of cytosolic Pex5p. A lesser but significant level of three RING peroxins was discernible in the organellar fraction of *pex1* ZP107 as compared with those of wild-type CHO-K1 (Fig. 6*C*, *bottom panels*, *lanes 1* and *2*). However, in *pex2* Z65 and *pex12* ZP109, RING peroxins, Pex10p plus Pex12p and Pex2p plus Pex10p, respectively were at a significantly lower or barely detectable level (Fig. 1*B*) (60) as well as in PBD fibroblasts (Fig. 1*C*). Taken together, these results strongly suggested that RING peroxins were indispensable for Cys-ubiquitination of Pex5p in mammalian cells, as in *S. cerevisiae* in which the RING finger of Pex12p and Pex2p mediated mono- and polyubiquitination of Pex5p, respectively (30).

Lys-linked Monoubiquitination of Pex5p Mainly Takes Place at Lys^{520}—To further investigate ubiquitin modification of Pex5p *in vivo*, we performed an immunoprecipitation assay using HEK cells transiently co-expressing N-terminally His- and FLAG-tagged Chinese hamster Pex5pL (HF-Pex5pL) (29) and HA_2-Ub. In whole cell lysates under the reducing conditions, immunoblotting with anti-His antibody visualized HF-Pex5pL in two bands: a major 90-kDa band (Fig. 7*A*, *middle top panels*, *lane 2*, *open arrowhead*) and a 95-kDa one (*solid arrowhead*), probably corresponding to those of endogenous, unmodified Pex5p and a Lys-linked ubiquitinated one, respectively, as detected with anti-Pex5p antibody (*top panel*, *lane 1* and Fig. 6, *A* and *B*). Although both bands of HF-Pex5pL were immunoprecipitated with anti-FLAG antibody (Fig. 7*A*, *first* and *second rows* of *panels*, *lane 6*), only the 95-kDa protein, and not the 90-kDa one, was cross-reactive with anti-ubiquitin antibody (*third row* of *panels*, *lane 6*, *solid arrowhead*). Co-expression of HA_2-Ub gave rise to an additional ubiquitin-positive band in the immunoprecipitate of HF-Pex5pL, indicative of HA_2-Ub-conjugated HF-Pex5pL (Fig. 7*A*, *first*, *second*, and *third rows* of *panels*, *lane 8*, *shaded arrowhead*). Similar Lys-linked ubiquitination of Pex5p was observed in CHO-K1 cells transiently expressing the shorter form of Pex5p as well as the longer form (Fig. 7*B*, *lanes 2*, *3*, *8*, and *9*). Taken together, these results strongly suggested that exogenously expressed Pex5p was, like endogenous Pex5p, covalently ubiquitinated.

As a step to delineating a role of Pex5p ubiquitination via a lysine residue, we attempted to determine the ubiquitination site(s) in Pex5pL. Ubiquitin-targeted lysine residues were not directly identified by mass spectrometric analysis (61) in tryptic digests of the modified form of HF-Pex5pL (Fig. 7*A*, *lane 6*), in which many peptide fragments derived from ubiquitin were indeed identified besides those from Pex5p (data not shown). Next, we constructed C-terminally HA-tagged Pex5pL (Pex5pL-HA) and its mutants with various numbers of Lys → Arg substitutions of, in total, 18 lysine residues and verified them for ubiquitination in CHO-K1 cells. In an immunoblot, the Lys-ubiquitinated, 95 kDa band of Pex5pL-HA was hardly detectable in CHO-K1 cells expressing several mutants containing K520R substitution and a K-less mutant with 18 Lys →

FIGURE 6. **Pex5p is ubiquitinated in both DTT-sensitive and -resistant manners *in vivo*.** *A*, DTT-sensitive and -resistant modifications of endogenous Pex5p in HEK cells. *Top panels*, PNS (*P*) fraction prepared from HEK cells in the absence (−) or presence (+) of 5 mM *N*-ethylmaleimide (*NEM*) was separated into the cytosolic (*C*) and organellar (*O*) fractions. An aliquot of C fraction equivalent to the P fraction and six aliquots of the O fraction were incubated in sample buffer in the absence (−) or presence (+) of 0.1 M DTT and analyzed by SDS-PAGE and immunoblotting with antibodies as indicated on the *left*. *Bottom panels*, HEK cells treated with the vehicle (−) or 10 μM MG132 (+) for 8 h were subjected to cell fractionation in the presence of 5 mM *N*-ethylmaleimide. An aliquot of the C fraction equivalent to six aliquots of the O fraction was analyzed as in the *top panels*. *Solid*, *shaded*, and *open arrowheads* indicate Pex5p with DTT-sensitive and -resistant modifications and unmodified Pex5p, respectively. *Dot*, an additional band of Pex5p with a DTT-resistant modification. *B*, Lys-linked ubiquitination of endogenous Pex5p. Endogenous Pex5p was pulled down with GST-Pex14pN260 from HEK cells transfected with mock (−) or a plasmid encoding HA_2-Ub (+) and was analyzed by SDS-PAGE in the presence of 0.1 M DTT followed by immunoblotting and Coomassie Brilliant Blue (*CBB*) staining. *Solid arrowheads*, Pex5pL covalently conjugated with HA_2-Ub via an isopeptide bond. *Solid* and *open dots*, GST-Pex14pN260 and GST, respectively. *C*, DTT-sensitive modification of Pex5p in CHO mutants. *Top panels*, PNS (*P*) fractions of CHO-K1 and peroxisome-deficient CHO cell mutants were separated into the cytosolic (*C*) and organelle (*O*) fractions and analyzed by SDS-PAGE and immunoblotting under non-reducing (*DTT* (−)) or reducing (*DTT* (+)) conditions as in *A*. An aliquot of the C fraction equivalent to the P fraction and eight aliquots of the O fraction were loaded. *Solid* and *open arrowheads*, Pex5p with DTT-sensitive modification and unmodified Pex5p, respectively. *Bottom panels*, expression of RING peroxins in O fractions in CHO-K1 and peroxisome-deficient CHO cell mutants was likewise analyzed by SDS-PAGE and immunoblotting with the antibodies indicated on the *left*. *Arrowheads* and *asterisks*, endogenous RING peroxins and nonspecific bands, respectively. *D*, DTT-sensitive modification of Pex5p in PBD patient fibroblasts. Equal aliquots of C and O fractions (*top*) or an aliquot of C fraction equivalent to the P fraction and eight aliquots of the O fraction (*other bottom panels*) prepared from control fibroblasts (control) and fibroblasts derived from PBD patients were analyzed by SDS-PAGE and immunoblotting as in *C*. *WB*, Western blot.

Arg mutations (Fig. 7*C*, *lanes 12–16*, *solid arrowhead*), whereas other variants showed the 95-kDa band as wild-type Pex5pL-HA (*lanes 2–11*). Only the K520R mutation gave rise to no Lys-ubiquitinated form of Pex5pL-HA, as shown with the K520R mutant (Fig. 7*B*, *lanes 5* and *11*) like the K-less mutant (*lanes 4* and *10*), suggesting that exogenously expressed Pex5pL was mainly ubiquitinated at Lys^{520}. Moreover, a KR mutant, 520K, where all lysine residues other than Lys^{520} were mutated to arginine showed a distinct 95-kDa band, like those noted with wild-type Pex5pS-HA and Pex5pL-HA at a lower level (Fig. 7*B*, *lanes 2*, *3*, *6*, *8*, *9*, and *12*, *solid arrowheads*), thereby supporting the specific ubiquitination of Pex5p at Lys^{520}.

Next, we verified Lys-ubiquitination of Pex5p in several peroxisome-deficient CHO cell mutants. A distinct ubiquitin-

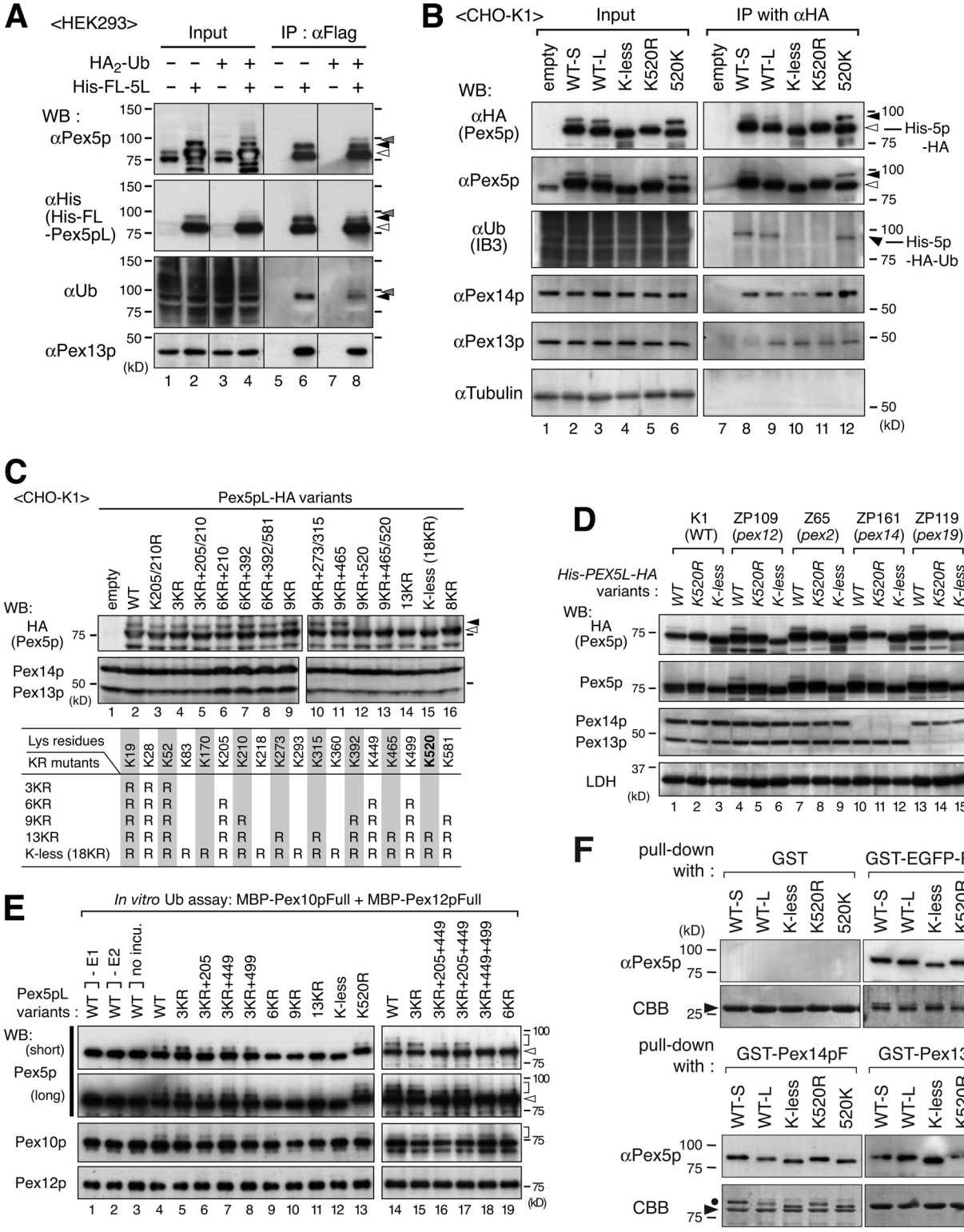

modified, 95-kDa protein band was detected in *pex12* ZP109, *pex2* Z65, *pex14* ZP161, *pex1* ZP107, and membrane assembly-defective *pex19* ZP119, each expressing wild-type Pex5pL-HA, at a higher level than in normal CHO-K1, whereas the 95-kDa band was not discernible in those expressing K520R and K-less mutants (Fig. 7*D*, *solid arrowhead*). These results suggested that Pex5p ubiquitination at Lys^{520} probably took place in the cytosol in a RING peroxin-independent manner. The Pex5pL-520K mutant was likewise ubiquitinated in *pex2* Z65, *pex12* ZP109, and *pex1* ZP107 (data not shown), supporting the cytosolic ubiquitination of Pex5p. In *pex10* fibroblasts derived from a complementation group B patient with Zellweger syndrome (43), Pex5p was expressed at a low level but slightly higher than that in fibroblasts from a control, where no apparently distinct Pex5p bands were discernible between these two types of cells (data not shown).

To investigate whether Pex10p directly ubiquitinates Lys^{520} of Pex5pL, various KR mutants of Pex5pL were verified by an *in vitro* ubiquitination assay using full-length Pex10p and Pex12p as in Fig. 4*C*. The Pex5pL-K520R mutant was ubiquitinated to the same extent as the wild type (Fig. 7*E*, *lanes 1–4* and *13*), hence suggesting that the Pex10p·Pex12p complex ubiquitinated Pex5pL not specifically at Lys^{520} but at other lysine residues, consistent with RING peroxin-independent ubiquitination of Pex5pL at Lys^{520} *in vivo* (Fig. 7*D*). Based on the results by thorough analyses using KR mutants, including 3KR, 6KR, 9KR, 13KR in which 3, 6, 9, and 13 lysine residues were respectively mutated to arginine as shown in Fig. 7*C*, *bottom panel*, and K-less mutants, it was most likely that the Pex10p·Pex12p E3 complex ubiquitinated Pex5pL preferentially at Lys^{449} and Lys^{499} (Fig. 7*E*). Essentially the same results were obtained from *in vitro* Pex5p ubiquitination assays using MBP-Pex10pC and MBP-Pex12pC (data not shown). We interpreted these results to mean that two different types of covalent ubiquitin modification have taken place in Pex5p: one at Lys^{520} by cytosolic unknown factor(s) in a peroxisome-independent manner and the other at multiple lysine residues except for Lys^{520} catalyzed by the Pex10p·Pex12p complex.

Ubiquitination of Pex5p via Lysine Residues Attenuates Its Export from Peroxisomes to the Cytosol—As a step to addressing a physiological role, if any, of the Lys ubiquitination of Pex5p, we investigated whether the ubiquitination modulates Pex5p interaction with its partners, including PTS1 cargoes and the docking complexes on peroxisomes, Pex14p and Pex13p. Upon immunoprecipitation of KR variants of Pex5pL-HA, Pex14p was co-immunoprecipitated at a relatively similar level as the wild-type Pex5pL-HA, His-Pex5pS-HA, and the K-less mutant (Fig. 7*B*, *lanes 8–12*). Pex13p was likewise co-immunoprecipitated with wild-type and KR mutants of Pex5pL-HA but not efficiently with His-Pex5pS-HA. Furthermore, in *in vitro* binding assays, the three Pex5pL KR mutants directly bound to Pex14p, Pex13p, and a PTS1 protein, indistinguishably from the wild-type Pex5pL and Pex5pS (Fig. 7*F*). These results suggested that the ubiquitination of Pex5p at Lys^{520} and possibly at other lysine residues did not alter Pex5p binding to the cargo proteins, Pex14p, and Pex13p.

Next, we investigated whether the Lys-ubiquitination in Pex5p is involved in the Pex5p shuttling between the cytosol and peroxisomes. In the *in vitro* Pex5p import assay (17) using ^{35}S-labeled Pex5pL and PNS fraction from *pex5* ZP139 cells (9), wild-type Pex5pL and its KR mutants, including K-less, K520R, and 520K, were detected at a similar level as a Proteinase K-resistant form (Fig. 8*A*, *top* and *bottom*, *lanes 5* and *10*), indicative of peroxisomal import (3, 17), hence suggesting that the Lys-ubiquitination of Pex5p was not involved in the import steps into peroxisomes, as well as the Cys-ubiquitination (29, 58). In *in vitro* Pex5p export assays using organelle-associated ^{35}S-Pex5pL (Fig. 8*A*, *lanes 3* and *8*), the amount of wild type and K520R of ^{35}S-Pex5pL decreased in the organellar fraction in a time-dependent manner, apparently with a concomitant increase in the level of both types of ^{35}S-Pex5pL in the cytosolic fraction (Fig. 8*B*, *left panels*), thereby demonstrating the export of wild-type and K520R-type ^{35}S-Pex5pL from peroxisomes. Such Pex5pL export was confirmed by verifying the sensitivity of the exported ^{35}S-Pex5pL variants to the treatment with Proteinase K (Fig. 8*B*, *right panels*). On the other hand, K-less and 520K mutants of ^{35}S-Pex5pL in the organellar fraction remained nearly at the same level throughout the export reaction in a Proteinase K-resistant form (Fig. 8*B*, *left* and *right panels*, *lanes 4–6* and *10–12*). The export efficiency of ^{35}S-Pex5pL variants was determined by taking the ratio of the respective ^{35}S-Pex5pL mutants in the cytosolic fraction (S) to those in the cytosol plus organellar fractions (S + P) (Fig. 8*C*). The export rates of K-less and 520K mutants were about two-

FIGURE 7. **Lys-linked monoubiquitination of Pex5p occurs at the Lys^{520} *in vivo*.** *A*, HEK cells were transfected with plasmids encoding His-FLAG-Pex5pL and HA_2-Ub as indicated at the *top*. Cells were cultured for 36 h and for an additional 2 h in the presence of MG132. His-FLAG-Pex5pL was immunoprecipitated with anti-FLAG IgG-agarose and analyzed by immunoblotting (*WB*) with the antibodies indicated on the *left*. *Input*, 10% cell lysates used for immunoprecipitation (*IP*). *Solid* and *shaded arrowheads*, His-FLAG-Pex5pL conjugated with endogenous ubiquitin and HA_2-Ub, respectively. *Open arrowhead*, unmodified His-FLAG-Pex5pL. *B*, CHO-K1 cells were transfected with plasmids encoding the shorter and longer forms of wild-type His-Pex5p-HA (*WT-S* and *WT-L*) and the KR mutants of the L form, K-less, K520R, and 520K. After a 1-day culture, cells were solubilized and subjected to immunoprecipitation with anti-HA antibody. Immunoprecipitates and the input (5%) were analyzed by SDS-PAGE under the reducing condition and immunoblotting as indicated on the *left*. *Solid* and *open arrowheads* indicate ubiquitinated and unmodified forms of His-Pex5p-HA variants, respectively. *Dots*, mouse IgG light chains, apparently weakly cross-reactive with anti-goat IgG secondary antibody. *C*, *top*, CHO-K1 was transfected with plasmids encoding wild-type Pex5pL-HA (WT) and the KR mutants and analyzed by SDS-PAGE and immunoblotting as in *B*. *Solid* and *open arrowheads*, ubiquitinated and unmodified forms of Pex5pL-HA variants, respectively. *Bottom*, *numerical diagram* of the Lys-to-Arg mutations in KR variants of Pex5pL-HA used in the *top*. *D*, KR mutants of Pex5p in peroxisome-deficient CHO mutants. Plasmids encoding wild-type Pex5pL-HA (*WT*) and the KR mutants were separately transfected to CHO-K1, *pex12* ZP109, *pex2* Z65, *pex14* ZP161, *pex19* ZP119, and *pex1* ZP107 cells. At 24 h post-transfection, cells were analyzed as in Fig. 7*B*. *Solid* and *open arrowheads*, Lys-ubiquitinated and unmodified forms of Pex5pL-HA mutants, respectively. The figure is shown as a composite of two separate experiments. *E*, the Pex10p·Pex12p complex preferentially ubiquitinates Lys^{449} and Lys^{499} in Pex5p *in vitro*. *Top*, *in vitro* ubiquitination assay was performed as in Fig. 5*C*, with MBP-fused full-length Pex10p and Pex12p, using various KR mutants of Pex5pL, as indicated at the *top*. A composite of two separate experiments (*lanes 1–13* and *14–19*) was shown. Lys-to-Arg mutations in KR variants of Pex5pL-HA are shown in the *bottom panel* of *C*. *F*, interaction between KR mutants of Pex5p and Pex5p-binding partners. Both S and L forms of wild-type Pex5p and KR mutants of Pex5pL were subjected to pull-down assays with GSH-Sepharose beads conjugated with GST, GST-EGFP-PTS1, GST-Pex14p, and GST-Pex13pN, respectively. Proteins in bound fractions were assessed by immunoblotting with anti-Pex5p antibody and by Coomassie Brilliant Blue (*CBB*) staining. *Solid arrowheads* indicate respective GST fusion proteins used for the assay. *Dot*, Pex5p variants recovered with GST-Pex14p.

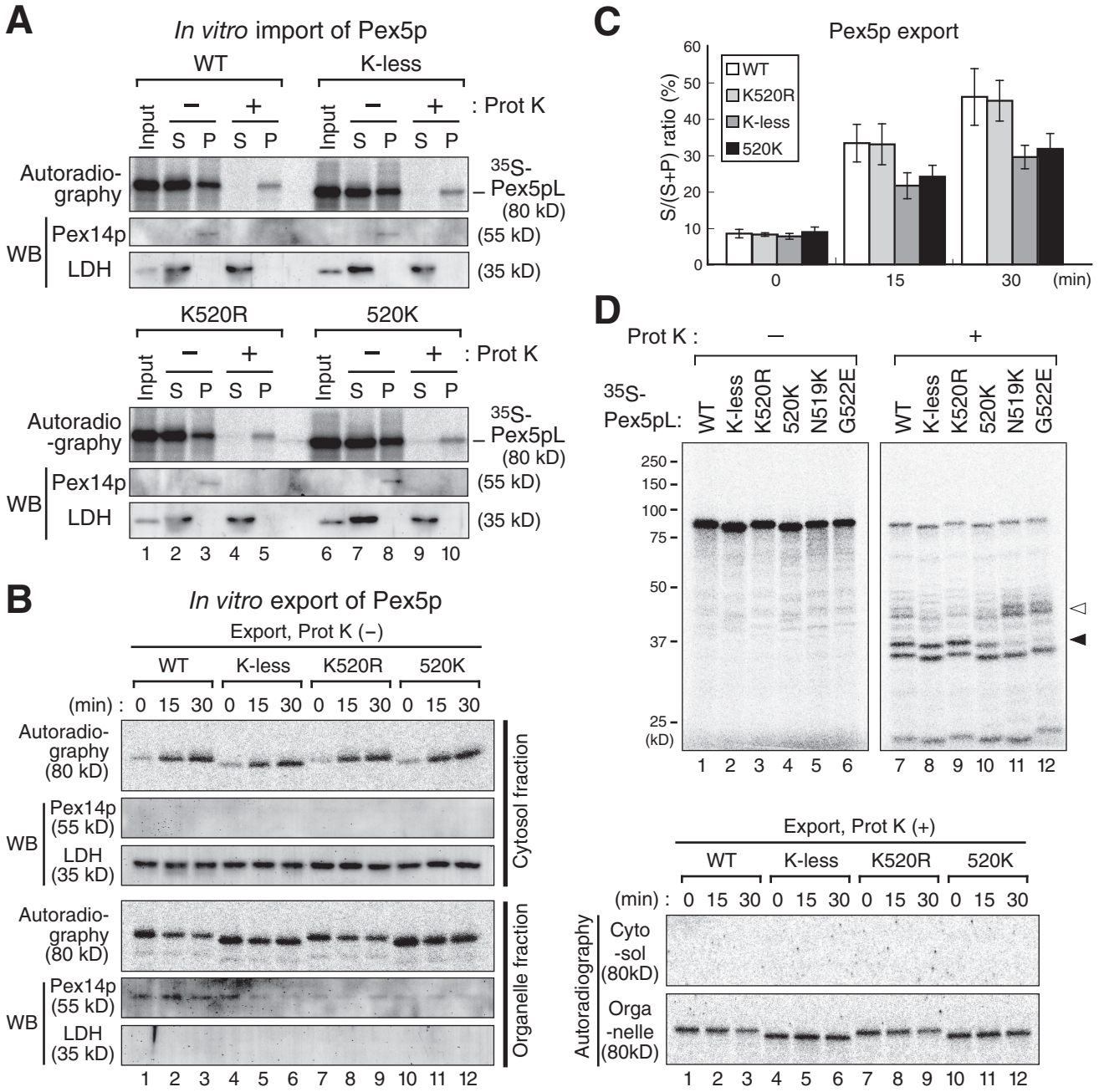

FIGURE 8. **KR mutation affects Pex5p export from but not import to peroxisomes.** *A*, import of KR mutants of Pex5p. An *in vitro* Pex5p import assay was performed with cell-free synthesized ^{35}S-Pex5pL variants and the PNS fraction of CHO *pex5* ZP105 in the absence of ATP as described under "Materials and Methods." After the import reaction, the reaction mixtures were mock-treated (−) or treated with 5 μg/ml Proteinase K (+) and separated into cytosolic (*S*) and organellar (*P*) fractions. Equal aliquots of total reaction mixtures (*Input*) and S and P fractions were analyzed by autoradiography and immunoblotting (*WB*) with antibodies to Pex14p and lactate dehydrogenase (*LDH*). Note that lactate dehydrogenase remained in the S fraction after the treatment with Proteinase K due to its resistance to Proteinase K (17). *B*, export of Pex5p KR mutants. Pex5p variants imported to peroxisomes (*lanes 3* and *8* in *A*) were verified for the export for 30 min at 26 °C. At each time point, the reaction mixtures were mock-treated (−, *left panels*) or treated with 5 μg/ml Proteinase K (+, *right panels*), fractionated, and analyzed as in *A*. *C*, quantification of the export of Pex5p variants. ^{35}S-Pex5pL variant bands, prior to the Proteinase K treatment after the export assays in *B*, were quantitated in three independent experiments. The ratios of ^{35}S-Pex5pL variants in the cytosolic fraction to those in the cytosolic plus organellar fractions were calculated and are represented as percentages with S.E. (*error bars*). *D*, proteolytic profiles of Pex5p KR mutants. Cell-free synthesized ^{35}S-Pex5pL variants were incubated on ice for 15 min in the absence (−, *left panel*) and presence (+, *right panel*) of 0.2 μg/ml Proteinase K (*Prot K*). The reaction mixtures were analyzed by SDS-PAGE and autoradiography. The N519K mutation in Chinese hamster Pex5pL corresponds to the N526K mutation in human Pex5pL identified in a *PEX5*-deficient PBD patient (8). G522E is a causal mutation in a *pex5* CHO mutant ZP139 (9). *Open* and *solid arrowheads* indicate the characteristic bands of 40 and 35 kDa, respectively.

thirds those of wild-type and K520R mutant (Fig. 8*C*). The absence of a readily visible difference between the ^{35}S-Pex5pL KR mutants in the cytosolic fraction was probably due to the ^{35}S-Pex5pL variants, including those associated with but not imported to peroxisomes as well as a nonspecifically bound one (3, 17). To address the possibility that KR mutations affect the conformation of Pex5p, KR mutants of Pex5pL were assessed by partial digestion with Proteinase K. When cell-free synthesized

wild-type ^{35}S-Pex5pL and its variants were incubated at a low concentration of Proteinase K, similar proteolytic fragment patterns were detectable between the wild-type Pex5pL and all of the KR mutants, K-less, K520R, and 520K (Fig. 8*D*, *lanes 7–10*). These band patterns were very similar to those of human normal Pex5pL after Proteinase K treatment, where three major protease-resistant bands were identified as the fragments containing the C-terminal TPR regions (62). On the other hand, PTS1 cargo did not bind to two Pex5pL mutants, one with the mutation N519K and the other with G522E, equivalent to human N526K of a PBD patient (8, 63) and a *pex5* CHO ZP139 (9), respectively. Upon digestion with Proteinase K of these two mutants, more distinct 42-kDa doublet bands (Fig. 8*D*, *lanes 11* and *12*, *open arrowhead*), but not the 35-kDa fragment (*solid arrowhead*), were detected. These proteolytic profiles were similar to that of human Pex5pL harboring N526K that caused the conformational change in the region preceding the C-terminal TPR domains (64). Given the finding that the K-less mutant of Pex5pL interacts with the PTS1 protein as well as Pex14p and Pex13p like wild-type Pex5p *in vitro* (Fig. 7*F*) and *in vivo* (Fig. 7*B*), the K-less and 520K mutants probably share the similar conformation with wild-type Pex5pL, whereas they are less efficiently exported from peroxisomes. Collectively, we interpreted these results to mean that the ubiquitination of Pex5p at multiple lysine residues, rather than at Lys^{520}, ensures the export of Pex5p from peroxisomes to cytosol, in addition to the prerequisite role of the ubiquitination at Cys^{11} in the export process (29, 58).

Next, we expressed KR mutants of Pex5pL in a *pex5* CHO mutant ZP139 and assessed their complementing activity. K520R and K-less mutants restored the impaired PTS1 protein import in ZP139, apparently with ~80 and 60% efficiency, respectively, as compared with wild-type Pex5pL (Fig. 9*B*, *left*). Moreover, these two KR mutants were more significantly lower, ~50 and ~20% of the wild type, in restoring the defective import of catalase (Fig. 9, *A* and *B*, *right*). The 520K mutant was similar to the K-less mutant in the complementing activity (Fig. 9, *A* and *B*), hence suggesting that ubiquitin modification of Pex5pL at Lys^{520} was dispensable for peroxisomal matrix protein import. Partial defects of K-less and 520K mutants in restoring the activity in peroxisomal matrix protein import (Fig. 9, *A* and *B*) were well correlated with their lower export efficiency (Fig. 8, *B* and *C*). It is more likely that the ubiquitination of Pex5p at multiple lysine residues besides Lys^{520} is required for the efficient protein import to peroxisomes. To obtain more insight into the role of Lys^{520} in Pex5p function, the 520K mutant yielding ubiquitination only at Lys^{520} was subjected to a pull-down assay. The ubiquitinated form of the 520K mutant expressed in the cytosol was defective in the interaction with GST-EGFP-PTS1, not GST-Pex14p (Fig. 9*C*, *lanes 1*, *3*, and *7*, *solid arrowhead*), whereas the unmodified 520K was recovered in the bound fraction of both GST-EGFP-PTS1 and GST-Pex14p with the same efficiency as a K-less mutant (*lanes 1–4*, *7*, and *8*, *open arrowhead*). These results indicated that ubiquitination of Pex5p at Lys^{520} specifically abrogates the binding of Pex5p to the PTS1 cargo protein, most likely in the cytosol (Fig. 7*D*). Therefore, Pex5p ubiquitination at Lys^{520} *in vivo* might play a role in self-inhibition of Pex5p in the cargo recognition in the cytosol rather than a regulatory one in the export process. However, we do not exclude the possibility that Lys^{520} of Pex5p plays a role in the peroxisomal protein import at unknown step(s) because K520R mutant is significantly low in the complementing activity (Figs. 9, *A* and *B*).

DISCUSSION

Identification as an E3 of Mammalian RING Peroxins—RING peroxins were postulated to function as a potential E3 about a decade ago (65, 66) by the analogy to the domain structure. Our *in vitro* ubiquitination assay using recombinant mammalian RING peroxins demonstrated that the RING finger of Pex10p and Pex2p, but not of Pex12p, self-ubiquitinated in the presence of the E2 enzymes UbcH5C and UbcH4 (Fig. 2). In contrast, all of the three RING fingers of RING peroxins in *S. cerevisiae* and *A. thaliana* exhibited E3 activity *in vitro* with both Pex4p and Ubc4 (30, 36) and human UbcH5B (38), respectively. Interestingly, Pex12p RING finger with no enzymatic activity significantly augments the E3 activity of Pex10p (Figs. 3 and 4), indicating that Pex12p functions as an accelerator of the Pex10p E3 enzyme. In *S. cerevisiae*, E3 activity was similarly enhanced by each of two pairs of RING peroxins, Pex10p·Pex12p and Pex10p·Pex2p, in a Pex4p- and Ubc4p-dependent manner, respectively (36). However, the situation is slightly different from the mammalian case because each RING finger of the three RING peroxins of *S. cerevisiae* and *A. thaliana* has E3 ligase activity (36, 38). Several RING finger proteins are known to function as heteromeric complexes, such as Mdm2·MdmX (67), BRCA1·BARD1 (68), and Ring1b·Bmi1 (69). In these heterocomplexes, each RING domain of MdmX, BARD1, and Bmi1 appears to lack the E3 activity (67–69). In the case of BRCA1·BARD1, BARD1 also structurally stabilizes the heterocomplex (70). These notions are consistent with the putative role of Pex12p in the mammalian Pex10p·Pex12p E3 complex. Yeast and mammalian RING peroxins share several properties, including that (i) the RING finger of Pex10p directly interacts with RING fingers of Pex2p and Pex12p (35, 36), and (ii) RING peroxins form a complex *in vivo*, and one RING peroxin is a prerequisite for the stable expression of the other two RING peroxins (Fig. 1) (30, 55, 71). These findings strongly support the notion that RING peroxins function as an E3 enzyme complex, whereas the specificity of E2 appears to vary in species. A typical RING finger peroxin, Pex2p, showed weak self-ubiquitination activity but no effects on the E3 activity of Pex10p in the absence and presence of Pex12p (Fig. 3). However, we do not exclude the possibility that an optimal E2, neither UbcH5C nor UbcH4, is required for the E3 activity, if any, of Pex2p and Pex12p.

Role of RING Peroxins in Pex5p Ubiquitination—We identified here that mammalian Pex5p is indeed monoubiquitinated at multiple lysine residues by the Pex10p·Pex12p complex in the presence of UbcH5C *in vitro*. Mutation in the Pex10p RING motif eliminated both the E3 activity and the peroxisome-restoring activity (Fig. 2, *B* and *D*), indicating an essential role of Pex10p-E3 activity in peroxisomal matrix protein import. Distinct roles of RING peroxins have been defined in yeast. *In vitro* ubiquitination assay showed that *S. cerevisiae* Pex12p catalyzes

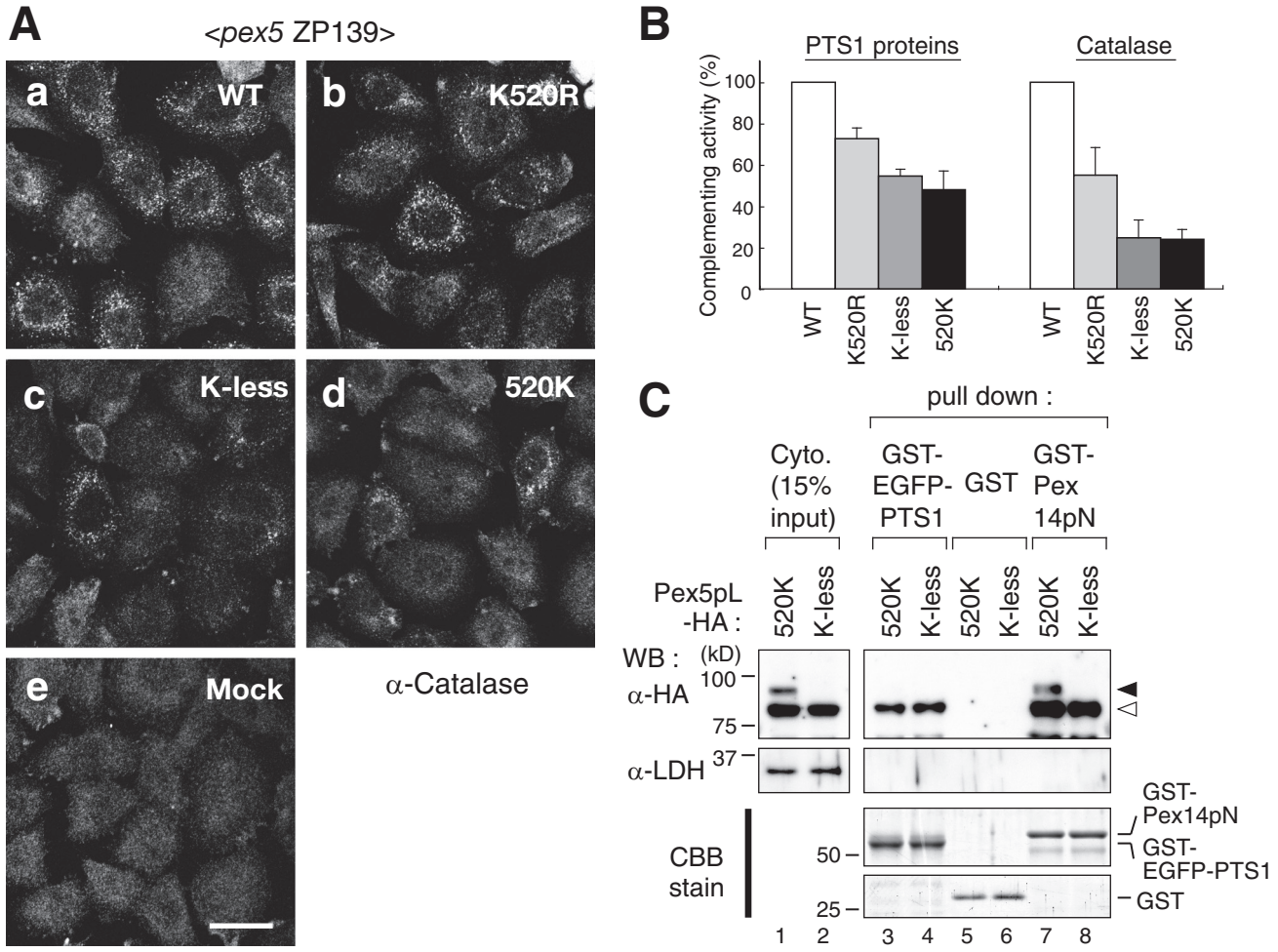

FIGURE 9. **Pex5p ubiquitination is involved in matrix protein import into peroxisomes.** *A*, complementing activity of Pex5pL KR mutants. CHO *pex5* ZP139 cells were transfected with plasmids, each encoding wild type, K520R, K-less, and 520K mutants of Pex5pL-HA. After a 1-day culture, cells were immunostained with anti-catalase antibody. *Bar*, 10 μm. *B*, quantification of complementing activity of KR mutants. Cells restored for the impaired import of PTS1 (not shown) and catalase (*A*) in 100–150 cells were counted in three independent experiments. Complementing activities of K520R, K-less, and 520K mutants were represented as percentages relative to that of wild-type with S.E. (*error bars*). *C*, ubiquitination at Lys^{520} abrogates the interaction of Pex5p with the PTS1 cargo protein. Cytosolic fractions of HEK cells expressing Pex5pL-HA mutants, 520K and K-less, were incubated with GSH-Sepharose beads conjugated with GST, GST-EGFP-PTS1, and GST-Pex14pN(1–260), respectively. Proteins in the bound fractions were analyzed as in Fig. 6*F* by immunoblotting, as indicated on the *left*, and staining with Coomassie Brilliant Blue (*CBB*). *Input*, 15% cytosolic fractions (*Cyto*) used for the pull-down assay (*lanes 1* and *2*). *Solid* and *open arrowheads*, 520K mutant ubiquitinated at Lys^{520} and unmodified forms of the 520K and K-less mutants, respectively.

Pex4p-dependent monoubiquitination of Pex5p (30), which is consistent with complete loss of the monoubiquitinated form of Pex5p in the Pex12p RING domain deletion mutant (30). Both *S. cerevisiae* Pex2p (30) and Pex10p (37) polyubiquitinate Pex5p *in vitro*, suggesting that they are E3s for polyubiquitination of Pex5p. Similarly, in *S. cerevisiae*, the PTS2 co-receptor, Pex18p, is mono- and polyubiquitinated by distinct pairs of E2/E3 enzymes: Pex4p plus Pex12p and Pex10p and Ubc4 plus Pex2p and Pex10p, respectively (72). We found that DTT-sensitive, Cys-monoubiquitination of Pex5p identified in wild-type CHO-K1 cells is impaired in the mutants *pex2* Z65 and *pex12* ZP109, where all three RING peroxins are unstable (Fig. 6*C*). Although the Pex10p·Pex12p complex is most likely a candidate for the yet undefined E3 in ubiquitination of mammalian Pex5p, the precise role(s) in the ubiquitination of Pex5p remains to be defined. In *P. pastoris*, all of the three RING peroxins are suggested to be required as E3 enzymes for mono- and polyubiquitination of Pex20p as well as Pex5p (26). Given the finding that RING peroxins form a complex *in vivo* (this study) (55, 71), three RING peroxins more likely act as a functional E3 unit, facilitating a variety of enzymatic activities, such as substrate specificity for Pex5p or Pex18p·Pex20p, the modes of ubiquitination (*i.e.* mono- or polyubiquitination), and the selection of E2 enzymes, Pex4p or Ubc4.

We found that Pex10p·Pex12p complex-mediated Lys-monoubiquitination of Pex5p is inhibited when bound to the initial Pex5p-docking site Pex14p and completely interfered with Pex14p and Pex5p cargo, PTS1 protein (Fig. 5*A*). In contrast, Pex5p bound to Pex13p is readily ubiquitinated as compared with free Pex5p, where the ubiquitinated Pex5p no longer binds to Pex13p (Fig. 5, *A* and *B*). Together with our earlier findings that Pex14p and Pex13p bind to cargo-loaded Pex5p and cargo-unloaded Pex5p, respectively (49), the Pex10p·Pex12p complex E3 most likely ubiquitinates Pex5p in the complex with Pex13p after being dissociated from the cargo and translocated from Pex14p, consistent with the reports that RING peroxins are located downstream of the Pex5p-cargo docking complex (14, 17, 55, 73).

Distinct Modes of Pex5p Ubiquitination and Function—Our data represent several differences in the mode of Pex5p ubiquitination between mammals and yeast. In *S. cerevisiae* mutants defective in later steps of the Pex5p translocation, polyubiquitinated forms of Pex5p accumulated in a Ubc4-dependent manner, leading to the degradation (19–23). On the other hand, mammalian Pex5p is monoubiquitinated by Pex10p·Pex12p E3 complex at multiple lysine residues (Fig. 4). This Lys-linked, monoubiquitinated form of Pex5p is most likely detected *in vivo* as a part of a DTT-resistant, slowly migrating band in the peroxisomal fraction in HEK cells (Fig. 6*A*) and MEF and RAW264.7 cells (data not shown). In contrast to the hardly detectable Lys-monoubiquitination of Pex5p in CHO-K1 cells, DTT-sensitive, Cys-ubiquitinated Pex5p distinctly accumulated in the peroxisomal fraction in several export-defective CHO mutants, including *pex1* ZP107, *pex6* ZP164, and *pex26* ZP167 (Fig. 6*C*), hence implying that in mammals, Lys-ubiquitination of Pex5p and its degradation are less frequent. This notion is supported by the finding that three lysines at positions 19, 28, and 53 in Chinese hamster Pex5p, which are positionally comparable with the polyubiquitinated lysine residues in yeast Pex5p (19, 20), are not likely to be ubiquitinated, based on the data that the KR mutant of the three lysines is indistinguishable from wild-type Pex5p in the ubiquitination assay (Fig. 7*E*) and in the protein stability in cells (Fig. 7*C*). Rather, three lysines at positions 205, 449, and 499, are preferentially monoubiquitinated (Fig. 7*E*). Furthermore, an export-deficient Pex5p-C11A mutant accumulates in peroxisomal membrane but display no ubiquitin modification (29), suggesting that Lys-ubiquitination-mediated degradation of Pex5p may occur at a minimum level under the physiological conditions of mammals. An *in vitro* Pex5p import/export system using rat peroxisomes identified a thiol-resistant modification of Pex5p with lower efficiency when an export-defective Pex5p(C11S) mutant was used, probably by conjugation to a lysine residue (57). This thiol-resistant ubiquitin modification of Pex5p(C11S) might be relevant to Lys-linked ubiquitination of Pex5p catalyzed by Pex10p·Pex12p complex-type E3 that we report here.

Physiological consequence of the Lys-monoubiquitination of Pex5p remains unknown in mammalian cells. We here provide for the first time several lines of evidence indicating that multiple monoubiquitination of Pex5p is involved in the export step from peroxisomes during its shuttling. This is deduced from the findings that KR mutants of Pex5p are retarded in their export from peroxisomes, not in the import (Fig. 8), and are less potent in restoring the impaired protein import in *pex5* cell mutants (Fig. 9). It is known that in yeast, monoubiquitination at a cysteine residue is essential for Pex5p-mediated protein import into peroxisomes (19, 20), whereas polyubiquitination at lysine residues is dispensable for the Pex5p function in peroxisome biogenesis (19, 20, 74). It is noteworthy, however, that either type of ubiquitin modification of yeast Pex5p is sufficient for the AAA peroxin-dependent dislocation of Pex5p from peroxisome membranes *in vitro* (20). Moreover, the Δ*ubc4*Δ*ubc5* mutant of *S. cerevisiae* shows a partial defect in the import of peroxisomal matrix proteins (23), implying that Ubc4-dependent, Lys-linked ubiquitination of Pex5p is probably involved in Pex5p recycling. In the case of mammalian Pex5p, Pex10p·Pex12p complex E3-catalyzed, most likely UbcH5C E2-dependent Lys-monoubiquitination plays an auxiliary role in the Pex5p export from peroxisomes, whereas in yeast, Pex5p Ubc4-dependent polyubiquitination confers no distinct functional role in peroxisome biogenesis. Moreover, we include the possibility that the Pex10p·Pex12p complex functions as an E3 for Cys-ubiquitination of Pex5p *in vivo*. Although no mammalian homologue of yeast Pex22p, a Pex4p-binding partner on the peroxisomal membrane, has yet been identified, the UbcH5 family of E2 enzymes is required for Cys-ubiquitination of Pex5p and the export reaction in the cell-free Pex5p import system (27), suggesting that the mammalian UbcH5 family is a functional homologue of yeast Pex4p. Indeed, in *PEX12*-deficient CHO mutants as well as *PEX10*-deficient fibroblasts from a PBD patient, Pex5p with no Cys-ubiquitination modification accumulates in the peroxisomal fraction (Fig. 6, *C* and *D*). Unsuccessful reconstitution of Cys-ubiquitination of mammalian Pex5p *in vitro* (Fig. 4*E*) may be due to the experimental conditions under which the reaction proceeds in solution, in contrast to the *in vivo* situation, where Pex5p locates as a membrane-bound form comprising a putative import machinery. A similar finding that the ubiquitination pattern differs between *in vitro* and *in vivo* conditions has been reported for the Pex4p- and Pex12p-mediated monoubiquitination of Pex5p that is detected as slowly migrating bands within a wide range *in vitro*, suggestive of ubiquitin modification at multiple sites (30). Together with our finding that UbcH5C-mediated and the Pex10p·Pex12p complex-catalyzed ubiquitination at lysines in mammalian Pex5p, it is likely that the UbcH5 family acts as E2 with dual roles in Pex5p ubiquitination in mammalian cells, functionally equivalent to Ubc4 and Pex4p in yeast.

The monoubiquitination of Lys^{520} in Pex5p that we identified is distinct as to where it takes place. Lys^{520} is monoubiquitin-modified in a manner independent of peroxisomal factors, including RING peroxins, apparently by a yet unidentified E3(s) in the cytosol (Fig. 7*D*). Lys^{520} in Chinese hamster Pex5pL is located in the N-terminal helix of the sixth tetratricopeptide repeat motif, corresponding to Lys^{527} in human Pex5pL, where the adjacent Asn^{526} is mutated in a *pex5* PBD patient with neonatal adrenoleukodystrophy, resulting in the compromised matrix protein import to peroxisomes (8, 75). Both Asn^{520} and Lys^{527} of human Pex5pL are located in the binding surface of the PTS1 motif (76). As expected from the structural information, ubiquitination of Pex5p at Lys^{520} abrogates the binding of Pex5p to PTS1 cargo protein (Fig. 9*C*), probably due to the physiological obstruction, whereas the K520R mutation itself shows no effect on the binding to the cargo (Fig. 7*F*). Therefore, Pex5p ubiquitination at Lys^{520} possibly self-inactivates to avoid a dominant negative effect when Pex5p becomes excess to the cargoes in the cytosol. Although Lys^{520} is not responsible for the export efficiency (Fig. 8, *A* and *B*), the complementing activity of the K520R mutant is significantly low (Fig. 9, *A* and *B*). Given that the K520R mutant is indistinguishable from wild-type Pex5p in the affinity to the binding partners (Fig. 7*F*), shuttling efficiency (Fig. 8, *A* and *B*), and structural conformation (Fig. 8*D*), either ubiquitination of Pex5p at Lys^{520} or the K520R mutation itself or, more likely, both affect the Pex5p function in

peroxisomal protein import. Interestingly, the lysine residue corresponding to Lys^{520} of Chinese hamster Pex5pL is completely conserved between Pex5p orthologues in vertebrates and *A. thaliana*, whereas the arginine residue instead of the lysine is conserved in fungi, *Caenorhabditis elegans*, and *Drosophila melanogaster* (data not shown). This partly explains the difference in lysine-linked ubiquitination between yeast and mammals in the ubiquitin-mediated regulation of Pex5p shuttling. Taken together, our findings shed light on the molecular mechanisms underlying Pex5p-mediated matrix protein import into peroxisomes and its regulation involving cellular homeostasis of peroxisomes.

Acknowledgments—We thank H. Yasuda and K. Tanaka for recombinant E1, K. Nakayama and S. Hatakeyama for plasmids encoding various E2s, and M. Matsumoto for mass spectrometry analysis and technical advice. We also thank S. Okuno for technical assistance, N. Akiyama for establishing the Z65/FLP2 cell line, M. Nishi and K. Shimizu for preparing figures, and members of the Fujiki laboratory for discussion.

REFERENCES

1. Lazarow, P. B., and Fujiki, Y. (1985) Biogenesis of peroxisomes. *Annu. Rev. Cell Biol.* **1,** 489–530
2. Gould, S. J., Keller, G.-A., Hosken, N., Wilkinson, J., and Subramani, S. (1989) A conserved tripeptide sorts proteins to peroxisomes. *J. Cell Biol.* **108,** 1657–1664
3. Miura, S., Kasuya-Arai, I., Mori, H., Miyazawa, S., Osumi, T., Hashimoto, T., and Fujiki, Y. (1992) Carboxyl-terminal consensus Ser-Lys-Leu-related tripeptide of peroxisomal proteins functions *in vitro* as a minimal peroxisome-targeting signal. *J. Biol. Chem.* **267,** 14405–14411
4. Osumi, T., Tsukamoto, T., Hata, S., Yokota, S., Miura, S., Fujiki, Y., Hijikata, M., Miyazawa, S., and Hashimoto, T. (1991) Amino-terminal presequence of the precursor of peroxisomal 3-ketoacyl-CoA thiolase is a cleavable signal peptide for peroxisomal targeting. *Biochem. Biophys. Res. Commun.* **181,** 947–954
5. Swinkels, B. W., Gould, S. J., Bodnar, A. G., Rachubinski, R. A., and Subramani, S. (1991) A novel, cleavable peroxisomal targeting signal at the amino-terminus of the rat 3-ketoacyl-CoA thiolase. *EMBO J.* **10,** 3255–3262
6. Fujiki, Y., Matsuzono, Y., Matsuzaki, T., and Fransen, M. (2006) Import of peroxisomal membrane proteins: the interplay of Pex3p- and Pex19p-mediated interactions. *Biochim. Biophys. Acta* **1763,** 1639–1646
7. Platta, H. W., and Erdmann, R. (2007) The peroxisomal protein import machinery. *FEBS Lett.* **581,** 2811–2819
8. Dodt, G., Braverman, N., Wong, C., Moser, A., Moser, H. W., Watkins, P., Valle, D., and Gould, S. J. (1995) Mutations in the PTS1 receptor gene, *PXR1*, define complementation group 2 of the peroxisome biogenesis disorders. *Nat. Genet.* **9,** 115–125
9. Otera, H., Okumoto, K., Tateishi, K., Ikoma, Y., Matsuda, E., Nishimura, M., Tsukamoto, T., Osumi, T., Ohashi, K., Higuchi, O., and Fujiki, Y. (1998) Peroxisome targeting signal type 1 (PTS1) receptor is involved in import of both PTS1 and PTS2: studies with *PEX5*-defective CHO cell mutants. *Mol. Cell Biol.* **18,** 388–399
10. Braverman, N., Steel, G., Obie, C., Moser, A., Moser, H., Gould, S. J., and Valle, D. (1997) Human *PEX7* encodes the peroxisomal PTS2 receptor and is responsible for rhizomelic chondrodysplasia punctata. *Nat. Genet.* **15,** 369–376
11. Motley, A. M., Hettema, E. H., Hogenhout, E. M., Brites, P., ten Asbroek, A. L., Wijburg, F. A., Baas, F., Heijmans, H. S., Tabak, H. F., Wanders, R. J., and Distel, B. (1997) Rhizomelic chondrodysplasia punctata is a peroxisomal protein targeting disease caused by a non-functional PTS2 receptor. *Nat. Genet.* **15,** 377–380
12. Purdue, P. E., Zhang, J. W., Skoneczny, M., and Lazarow, P. B. (1997) Rhizomelic chondrodysplasia punctata is caused by deficiency of human *PEX7*, a homologue of the yeast PTS2 receptor. *Nat. Genet.* **15,** 381–384
13. Albertini, M., Rehling, P., Erdmann, R., Girzalsky, W., Kiel, J. A., Veenhuis, M., and Kunau, W.-H. (1997) Pex14p, a peroxisomal membrane protein binding both receptors of the two PTS-dependent import pathways. *Cell* **89,** 83–92
14. Otera, H., Harano, T., Honsho, M., Ghaedi, K., Mukai, S., Tanaka, A., Kawai, A., Shimizu, N., and Fujiki, Y. (2000) The mammalian peroxin Pex5pL, the longer isoform of the mobile peroxisome targeting signal (PTS) type 1 transporter, translocates Pex7p-PTS2 protein complex into peroxisomes via its initial docking site, Pex14p. *J. Biol. Chem.* **275,** 21703–21714
15. Saidowsky, J., Dodt, G., Kirchberg, K., Wegner, A., Nastainczyk, W., Kunau, W.-H., and Schliebs, W. (2001) The di-aromatic pentapeptide repeats of the human peroxisome import receptor PEX5 are separate high affinity binding sites for the peroxisomal membrane protein PEX14. *J. Biol. Chem.* **276,** 34524–34529
16. Platta, H. W., Grunau, S., Rosenkranz, K., Girzalsky, W., and Erdmann, R. (2005) Functional role of the AAA peroxins in dislocation of the cycling PTS1 receptor back to the cytosol. *Nat. Cell Biol.* **7,** 817–822
17. Miyata, N., and Fujiki, Y. (2005) Shuttling mechanism of peroxisome targeting signal type 1 receptor Pex5: ATP-independent import and ATP-dependent export. *Mol. Cell Biol.* **25,** 10822–10832
18. Weissman, A. M., Shabek, N., and Ciechanover, A. (2011) The predator becomes the prey: regulating the ubiquitin system by ubiquitylation and degradation. *Nat. Rev. Mol. Cell Biol.* **12,** 605–620
19. Williams, C., van den Berg, M., Sprenger, R. R., and Distel, B. (2007) A conserved cysteine is essential for Pex4p-dependent ubiquitination of the peroxisomal import receptor Pex5p. *J. Biol. Chem.* **282,** 22534–22543
20. Platta, H. W., El Magraoui, F., Schlee, D., Grunau, S., Girzalsky, W., and Erdmann, R. (2007) Ubiquitination of the peroxisomal import receptor Pex5p is required for its recycling. *J. Cell Biol.* **177,** 197–204
21. Kiel, J. A., Emmrich, K., Meyer, H. E., and Kunau, W.-H. (2005) Ubiquitination of the peroxisomal targeting signal type 1 receptor, Pex5p, suggests the presence of a quality control mechanism during peroxisomal matrix protein import. *J. Biol. Chem.* **280,** 1921–1930
22. Kragt, A., Voorn-Brouwer, T., van den Berg, M., and Distel, B. (2005) The *Saccharomyces cerevisiae* peroxisomal import receptor Pex5p is monoubiquitinated in wild type cells. *J. Biol. Chem.* **280,** 7867–7874
23. Platta, H. W., Girzalsky, W., and Erdmann, R. (2004) Ubiquitination of the peroxisomal import receptor Pex5p. *Biochem. J.* **384,** 37–45
24. Hensel, A., Beck, S., El Magraoui, F., Platta, H. W., Girzalsky, W., and Erdmann, R. (2011) Cysteine-dependent ubiquitination of Pex18p is linked to cargo translocation across the peroxisomal membrane. *J. Biol. Chem.* **286,** 43495–43505
25. Léon, S., Zhang, L., McDonald, W. H., Yates, J., 3rd, Cregg, J. M., and Subramani, S. (2006) Dynamics of the peroxisomal import cycle of PpPex20p: ubiquitin-dependent localization and regulation. *J. Cell Biol.* **172,** 67–78
26. Liu, X., and Subramani, S. (2013) Unique requirements for mono- and polyubiquitination of the peroxisomal targeting signal co-receptor, Pex20. *J. Biol. Chem.* **288,** 7230–7240
27. Grou, C. P., Carvalho, A. F., Pinto, M. P., Wiese, S., Piechura, H., Meyer, H. E., Warscheid, B., Sá-Miranda, C., and Azevedo, J. E. (2008) Members of the E2D (UbcH5) family mediate the ubiquitination of the conserved cysteine of Pex5p, the peroxisomal import receptor. *J. Biol. Chem.* **283,** 14190–14197
28. Grou, C. P., Carvalho, A. F., Pinto, M. P., Huybrechts, S. J., Sá-Miranda, C., Fransen, M., and Azevedo, J. E. (2009) Properties of the ubiquitin-Pex5p thiol ester conjugate. *J. Biol. Chem.* **284,** 10504–10513
29. Okumoto, K., Misono, S., Miyata, N., Matsumoto, Y., Mukai, S., and Fujiki, Y. (2011) Cysteine ubiquitination of PTS1 receptor Pex5p regulates Pex5p recycling. *Traffic* **12,** 1067–1083
30. Platta, H. W., El Magraoui, F., Bäumer, B. E., Schlee, D., Girzalsky, W., and Erdmann, R. (2009) Pex2 and Pex12 function as protein-ubiquitin ligases in peroxisomal protein import. *Mol. Cell Biol.* **29,** 5505–5516
31. Deshaies, R. J., and Joazeiro, C. A. (2009) RING domain E3 ubiquitin ligases. *Annu. Rev. Biochem.* **78,** 399–434

32. Weller, S., Gould, S. J., and Valle, D. (2003) Peroxisome biogenesis disorders. *Annu. Rev. Genomics Hum. Genet.* **4,** 165–211
33. Dodt, G., and Gould, S. J. (1996) Multiple PEX genes are required for proper subcellular distribution and stability of Pex5p, the PTS1 receptor: evidence that PTS1 protein import is mediated by a cycling receptor. *J. Cell Biol.* **135,** 1763–1774
34. Chang, C.-C., Warren, D. S., Sacksteder, K. A., and Gould, S. J. (1999) PEX12 interacts with PEX5 and PEX10 and acts downstream of receptor docking in peroxisomal matrix protein import. *J. Cell Biol.* **147,** 761–774
35. Okumoto, K., Abe, I., and Fujiki, Y. (2000) Molecular anatomy of the peroxin Pex12p: RING finger domain is essential for Pex12p function and interacts with the peroxisome-targeting signal type 1-receptor Pex5p and a RING peroxin, Pex10p. *J. Biol. Chem.* **275,** 25700–25710
36. El Magraoui, F., Bäumer, B. E., Platta, H. W., Baumann, J. S., Girzalsky, W., and Erdmann, R. (2012) The RING-type ubiquitin ligases Pex2p, Pex10p and Pex12p form a heteromeric complex that displays enhanced activity in an ubiquitin conjugating enzyme-selective manner. *FEBS J.* **279,** 2060–2070
37. Williams, C., van den Berg, M., Geers, E., and Distel, B. (2008) Pex10p functions as an E_3 ligase for the Ubc4p-dependent ubiquitination of Pex5p. *Biochem. Biophys. Res. Commun.* **374,** 620–624
38. Kaur, N., Zhao, Q., Xie, Q., and Hu, J. (2013) *Arabidopsis* RING peroxins are E3 ubiquitin ligases that interact with two homologous ubiquitin receptor proteins. *J. Integr. Plant Biol.* **55,** 108–120
39. Tsukamoto, T., Yokota, S., and Fujiki, Y. (1990) Isolation and characterization of Chinese hamster ovary cell mutants defective in assembly of peroxisomes. *J. Cell Biol.* **110,** 651–660
40. Okumoto, K., Shimozawa, N., Kawai, A., Tamura, S., Tsukamoto, T., Osumi, T., Moser, H., Wanders, R. J., Suzuki, Y., Kondo, N., and Fujiki, Y. (1998) PEX12, the pathogenic gene of group III Zellweger syndrome: cDNA cloning by functional complementation on a CHO cell mutant, patient analysis, and characterization of Pex12p. *Mol. Cell Biol.* **18,** 4324–4336
41. Matsumoto, N., Tamura, S., Furuki, S., Miyata, N., Moser, A., Shimozawa, N., Moser, H. W., Suzuki, Y., Kondo, N., and Fujiki, Y. (2003) Mutations in novel peroxin gene *PEX26* that cause peroxisome-biogenesis disorders of complementation group 8 provide a genotype-phenotype correlation. *Am. J. Hum. Genet.* **73,** 233–246
42. Okumoto, K., and Fujiki, Y. (1997) PEX12 encodes an integral membrane protein of peroxisomes. *Nat. Genet.* **17,** 265–266
43. Okumoto, K., Itoh, R., Shimozawa, N., Suzuki, Y., Tamura, S., Kondo, N., and Fujiki, Y. (1998) Mutation in *PEX10* is the cause of Zellweger peroxisome deficiency syndrome of complementation group B. *Hum. Mol. Genet.* **7,** 1399–1405
44. Shimozawa, N., Tsukamoto, T., Suzuki, Y., Orii, T., Shirayoshi, Y., Mori, T., and Fujiki, Y. (1992) A human gene responsible for Zellweger syndrome that affects peroxisome assembly. *Science* **255,** 1132–1134
45. Tamura, S., Okumoto, K., Toyama, R., Shimozawa, N., Tsukamoto, T., Suzuki, Y., Osumi, T., Kondo, N., and Fujiki, Y. (1998) Human *PEX1* cloned by functional complementation on a CHO cell mutant is responsible for peroxisome-deficient Zellweger syndrome of complementation group I. *Proc. Natl. Acad. Sci. U.S.A.* **95,** 4350–4355
46. Fukuda, S., Shimozawa, N., Suzuki, Y., Zhang, Z., Tomatsu, S., Tsukamoto, T., Hashiguchi, N., Osumi, T., Masuno, M., Imaizumi, K., Kuroki, Y., Fujiki, Y., Orii, T., and Kondo, N. (1996) Human peroxisome assembly factor-2 (PAF-2): a gene responsible for group C peroxisome biogenesis disorder in humans. *Am. J. Hum. Genet.* **59,** 1210–1220
47. Honsho, M., Tamura, S., Shimozawa, N., Suzuki, Y., Kondo, N., and Fujiki, Y. (1998) Mutation in *PEX16* is causal in the peroxisome-deficient Zellweger syndrome of complementation group D. *Am. J. Hum. Genet.* **63,** 1622–1630
48. Harano, T., Shimizu, N., Otera, H., and Fujiki, Y. (1999) Transmembrane topology of the peroxin, Pex2p, an essential component for the peroxisome assembly. *J. Biochem.* **125,** 1168–1174
49. Otera, H., Setoguchi, K., Hamasaki, M., Kumashiro, T., Shimizu, N., and Fujiki, Y. (2002) Peroxisomal targeting signal receptor Pex5p interacts with cargoes and import machinery components in a spatiotemporally differentiated manner: conserved Pex5p WXXXF/Y motifs are critical for matrix protein import. *Mol. Cell Biol.* **22,** 1639–1655
50. Itoh, R., and Fujiki, Y. (2006) Functional domains and dynamic assembly of the peroxin Pex14p, the entry site of matrix proteins. *J. Biol. Chem.* **281,** 10196–10205
51. Tsukamoto, T., Miura, S., and Fujiki, Y. (1991) Restoration by a 35K membrane protein of peroxisome assembly in a peroxisome-deficient mammalian cell mutant. *Nature* **350,** 77–81
52. Akiyama, N., Ghaedi, K., and Fujiki, Y. (2002) A novel *pex2* mutant: catalase-deficient but temperature-sensitive PTS1 and PTS2 import. *Biochem. Biophys. Res. Commun.* **293,** 1523–1529
53. Toyama, R., Mukai, S., Itagaki, A., Tamura, S., Shimozawa, N., Suzuki, Y., Kondo, N., Wanders, R. J., and Fujiki, Y. (1999) Isolation, characterization, and mutation analysis of *PEX13*-defective Chinese hamster ovary cell mutants. *Hum. Mol. Genet.* **8,** 1673–1681
54. Shimizu, N., Itoh, R., Hirono, Y., Otera, H., Ghaedi, K., Tateishi, K., Tamura, S., Okumoto, K., Harano, T., Mukai, S., and Fujiki, Y. (1999) The peroxin Pex14p: cDNA cloning by functional complementation on a Chinese hamster ovary cell mutant, characterization, and functional analysis. *J. Biol. Chem.* **274,** 12593–12604
55. Hazra, P. P., Suriapranata, I., Snyder, W. B., and Subramani, S. (2002) Peroxisome remnants in *pex3*Δ cells and the requirement of Pex3p for interactions between the peroxisomal docking and translocation subcomplexes. *Traffic* **3,** 560–574
56. Warren, D. S., Morrell, J. C., Moser, H. W., Valle, D., and Gould, S. J. (1998) Identification of *PEX10*, the gene defective in complementation group 7 of the peroxisome-biogenesis disorders. *Am. J. Hum. Genet.* **63,** 347–359
57. Carvalho, A. F., Pinto, M. P., Grou, C. P., Alencastre, I. S., Fransen, M., Sá-Miranda, C., and Azevedo, J. E. (2007) Ubiquitination of mammalian Pex5p, the peroxisomal import receptor. *J. Biol. Chem.* **282,** 31267–31272
58. Miyata, N., Okumoto, K., Mukai, S., Noguchi, M., and Fujiki, Y. (2012) AWP1/ZFAND6 functions in Pex5 export by interacting with Cys-monoubiquitinated Pex5 and Pex6 AAA ATPase. *Traffic* **13,** 168–183
59. Ellison, M. J., and Hochstrasser, M. (1991) Epitope-tagged ubiquitin. A new probe for analyzing ubiquitin function. *J. Biol. Chem.* **266,** 21150–21157
60. Noguchi, M., Okumoto, K., and Fujiki, Y. (2013) System to quantify the import of peroxisomal matrix proteins by fluorescence intensity. *Genes Cells* **18,** 476–492
61. Matsumoto, M., Hatakeyama, S., Oyamada, K., Oda, Y., Nishimura, T., and Nakayama, K. I. (2005) Large-scale analysis of the human ubiquitin-related proteome. *Proteomics* **5,** 4145–4151
62. Costa-Rodrigues, J., Carvalho, A. F., Fransen, M., Hambruch, E., Schliebs, W., Sá-Miranda, C., and Azevedo, J. E. (2005) Pex5p, the peroxisomal cycling receptor, is a monomeric non-globular protein. *J. Biol. Chem.* **280,** 24404–24411
63. Gatto, G. J., Jr., Geisbrecht, B. V., Gould, S. J., and Berg, J. M. (2000) Peroxisomal targeting signal-1 recognition by the TPR domains of human PEX5. *Nat. Struct. Biol.* **7,** 1091–1095
64. Carvalho, A. F., Grou, C. P., Pinto, M. P., Alencastre, I. S., Costa-Rodrigues, J., Fransen, M., Sá-Miranda, C., and Azevedo, J. E. (2007) Functional characterization of two missense mutations in Pex5p: C11S and N526K. *Biochim. Biophys. Acta* **1773,** 1141–1148
65. Freemont, P. S. (2000) Ubiquitination: RING for destruction? *Curr. Biol.* **10,** R84–R87
66. Lazarow, P. B. (2003) Peroxisome biogenesis: advances and conundrums. *Curr. Opin. Cell Biol.* **15,** 489–497
67. Badciong, J. C., and Haas, A. L. (2002) MdmX is a RING Finger ubiquitin ligase capable of synergistically enhancing Mdm2 ubiquitination. *J. Biol. Chem.* **277,** 49668–49675
68. Hashizume, R., Fukuda, M., Maeda, I., Nishikawa, H., Oyake, D., Yabuki, Y., Ogata, H., and Ohta, T. (2001) The RING heterodimer BRCA1-BARD1 is a ubiquitin ligase inactivated by a breast cancer-derived mutation. *J. Biol. Chem.* **276,** 14537–14540
69. Wang, H., Wang, L., Erdjument-Bromage, H., Vidal, M., Tempst, P., Jones, R. S., and Zhang, Y. (2004) Role of histone H2A ubiquitination in Polycomb silencing. *Nature* **431,** 873–878
70. Brzovic, P. S., Keeffe, J. R., Nishikawa, H., Miyamoto, K., Fox, D., 3rd, Fukuda, M., Ohta, T., and Klevit, R. (2003) Binding and recognition in the

assembly of an active BRCA1/BARD1 ubiquitin-ligase complex. *Proc. Natl. Acad. Sci. U.S.A.* **100,** 5646–5651
71. Agne, B., Meindl, N. M., Niederhoff, K., Einwächter, H., Rehling, P., Sickmann, A., Meyer, H. E., Girzalsky, W., and Kunau, W.-H. (2003) Pex8p: an intraperoxisomal organizer of the peroxisomal import machinery. *Mol. Cell* **11,** 635–646
72. El Magraoui, F., Brinkmeier, R., Schrötter, A., Girzalsky, W., Müller, T., Marcus, K., Meyer, H., Erdmann, R., and Platta, H. W. (2013) Distinct ubiquitination cascades act on the peroxisomal targeting signal type 2 co-receptor Pex18p. *Traffic* **14,** 1290–1301
73. Collins, C. S., Kalish, J. E., Morrell, J. C., McCaffery, J. M., and Gould, S. J. (2000) The peroxisome biogenesis factors Pex4p, Pex22p, Pex1p, and Pex6p act in the terminal steps of peroxisomal matrix protein import. *Mol. Cell Biol.* **20,** 7516–7526
74. Kiel, J. A., Otzen, M., Veenhuis, M., and van der Klei, I. J. (2005) Obstruction of polyubiquitination affects PTS1 peroxisomal matrix protein import. *Biochim. Biophys. Acta* **1745,** 176–186
75. Shimozawa, N., Zhang, Z., Suzuki, Y., Imamura, A., Tsukamoto, T., Osumi, T., Fujiki, Y., Orii, T., Barth, P. G., Wanders, R. J., and Kondo, N. (1999) Functional heterogeneity of C-terminal peroxisome targeting signal 1 in *PEX5*-defective patients. *Biochem. Biophys. Res. Commun.* **262,** 504–508
76. Stanley, W. A., Filipp, F. V., Kursula, P., Schüller, N., Erdmann, R., Schliebs, W., Sattler, M., and Wilmanns, M. (2006) Recognition of a functional peroxisome type 1 target by the dynamic import receptor Pex5p. *Mol. Cell* **24,** 653–663